

Defect-Mediated Trafficking across Cell Membranes: Insights from *in Silico* Modeling

Andrey A. Gurtovenko,^{*,†} Jamshed Anwar,[‡] and Ilpo Vattulainen^{§,||,⊥}

Institute of Macromolecular Compounds, Russian Academy of Sciences, Bolshoi Prospect 31, V.O., St. Petersburg, 199004 Russia, Computational Laboratory, Institute of Pharmaceutical Innovation, University of Bradford, Bradford, West Yorkshire BD7 1DP, U.K., Department of Physics, Tampere University of Technology, P.O. Box 692, FI-33101 Tampere, Finland, Aalto University, School of Science and Technology, Finland, and MEMPHYS—Center for Biomembrane Physics, University of Southern Denmark, Odense, Denmark

Received March 4, 2010

Contents

1. Introduction	6077
2. Molecular Dynamics Simulations of Lipid Bilayers	6079
3. Formation of Transient Defects in Lipid Membranes	6080
3.1. Metastable Water Pores during Lipid Self-Assembly	6080
3.2. Electroporation	6081
3.3. Tension-Induced Pores	6083
3.4. Water Pores Induced by Shock Waves	6084
3.5. Membrane Defects Induced by Surface-Active Molecules	6085
3.6. Peptide-Induced Poration of Membranes	6087
3.7. Pore Formation Induced by Cationic Polymers	6089
3.8. Pore Formation due to Lipid Peroxidation	6091
3.9. Energetics of Pore Formation in Lipid Membranes	6091
4. Trafficking of Salt Ions across Protein-Free Lipid Membranes	6093
4.1. Defect-Mediated Ion Permeation without Actual Pore Formation	6094
4.2. Ion Transport through Preformed Water Pores	6095
5. Transmembrane Lipid Translocation (Flip-Flop)	6096
5.1. Energetics of Lipid Transmembrane Translocation	6096
5.2. Pore-Mediated Lipid Translocation (Flip-Flop)	6097
6. Polyelectrolyte Trafficking across Lipid Membranes	6098
7. Conclusions	6099
8. Acknowledgments	6100
9. References	6100



Andrey Gurtovenko is a Senior Researcher at the Institute of Macromolecular Compounds, Russian Academy of Sciences, St. Petersburg, Russia. He graduated from St. Petersburg State University (Russia), where he was trained as a theoretical physicist. After receiving his Ph.D. from the Institute of Macromolecular Compounds in 1999, he spent several years working in the Theoretical Polymer Group of Prof. A. Blumen (University of Freiburg, Germany), in the Biophysics and Soft Matter Group of Prof. I. Vattulainen (Helsinki University of Technology, Finland), and in the Computational Biophysics Group of Prof. J. Anwar (University of Bradford, U.K.). His current research interests include biomolecular modeling, membrane biophysics, drug and gene delivery, and polymer nanocomposites. Andrey Gurtovenko is a recipient of a Bessel Research Award 2010 (Alexander von Humboldt Foundation, Germany).

to each other in a tail-to-tail fashion, so that their hydrophilic headgroups are located on the bilayer surface and therefore are in direct contact with aqueous solution. The hydrocarbon nonpolar chains of lipid molecules are hidden inside the bilayer, forming the membrane hydrophobic core. Membrane proteins are either embedded in the lipid bilayer matrix or attached to its surface.²

The cell membrane, being a site of complex interactions involving lipids, membrane proteins, and small solutes solvated in the cellular fluid, serves as a hub in mediating numerous cellular functions. One of the important ones is trafficking of various substances, i.e. transport of molecules from the cytoplasm to the extracellular fluid and vice versa.² In living cells the internal structure of cell membranes dictates their permeability properties. Because of the hydrophobic interior of lipid bilayers, small nonpolar molecules can permeate cell membranes rather easily. In contrast, the transmembrane transport of hydrophilic molecules and salt ions requires specialized membrane proteins such as ionic channels and transporters. There are, however, numerous experimental indications that membrane trafficking can also

1. Introduction

All living cells are surrounded by plasma membranes that separate the cell interior from the extracellular environment and are responsible for the selective permeability of cells.¹ The cell membrane is a complex structure and consists mainly of lipids, proteins, and carbohydrates. Lipid molecules, being amphiphilic in nature, are organized in a well-known bilayer structure: Two layers of lipids are adjacent

* Corresponding author. E-mail: a.gurtovenko@gmail.com. Web: biosimu.org.

[†] Russian Academy of Sciences.

[‡] University of Bradford.

[§] Tampere University of Technology.

^{||} Aalto University.

[⊥] University of Southern Denmark.



Jamshed Anwar is a Professor of Computational Pharmaceutical Sciences at the Institute of Pharmaceutical Innovation (IPI), University of Bradford, and a Director of Research for the Bradford School of Pharmacy and the IPI. His research field is molecular simulation and statistical thermodynamics of organic solids and soft matter, with a particular emphasis on pharmaceuticals and drug delivery. Specific areas include simulation of biological lipid membranes as well as their interaction with drug delivery systems; phase behavior in solids with applications in crystal engineering, phase transformations in crystals, and stability; and generation of nanocrystals. Anwar has a degree in Pharmacy and a Ph.D. in Chemical Physics/Crystallography from Birkbeck College London, University of London. Prior to his appointment at the IPI, he was a Reader in the Molecular Biophysics Group at King's College London. He has also spent periods at the University of Pennsylvania, the Institute of Atomic & Molecular Physics (AMOLF) in The Netherlands, and Cambridge University. Earlier in his career he held a Laboratory Leader's position with Glaxo Group Research (now GSK). He is a recipient of the RP Scherer Award (1986) and the Pfizer Award (1999).



Ilpo Vattulainen (born 1968) defended his Ph.D. thesis at Helsinki University of Technology in 1998 and then moved to the MEMPHYS group in Denmark for a Marie Curie Fellowship. He founded the Biological Physics group in 2001 and was awarded a 5-year fellowship by the Academy of Finland for 2002–2007. In 2006 he was appointed to a professorship in biological physics at Tampere University of Technology. His group of about 25 people is affiliated to two centers of excellence, one in Finland and another in Denmark. The group focuses on computational and theoretical studies of phenomena dealing with biomembranes, proteins, drugs, sterols, carbohydrates, and nanomaterials. He loves trains and good food, especially sushi and champagne.

take place unassisted through transient membrane defects that include water pores.

The interest in defect-mediated trafficking across cell membranes is, in general, twofold, because of its physiological relevance³ and because this activity can be modulated for some important biomedical and biotechnological applications. First of all, formation of transient defects in cell membranes and defect-mediated transport of solutes across

membranes has clear biological relevance. For instance, trafficking of ions through cell membranes is central to many cellular processes and functions. It is well established that, in addition to active protein-mediated transport, ions and other small hydrophilic molecules can leak in small amounts across a membrane unassisted.^{4–6} Since entrance of charged salt ions into the hydrophobic membrane core is energetically very unfavorable, a possible molecular mechanism of passive ion permeation could involve formation of transient water pores that reduce the permeation barrier and greatly facilitate ionic transport. This pore-mediated ion leakage is believed to be the dominant pathway for cations in sufficiently thin lipid membranes.^{7–10} Such an unassisted ion transport is of much interest, since cell membranes strive to maintain the ionic electrochemical gradient, which is important for a variety of activities, such as ATP synthesis, transport of nutrients, and conveyance of electrical signals. Thus, any ion leakage across the membrane is coupled to energy transduction and therefore to cellular function.

Another type of biologically relevant trafficking is the translocation of lipid molecules across membranes (lipid flip-flop). In general, membranes of most animal cells are asymmetric with regard to transmembrane distribution of lipids across the membrane.^{11,12} This asymmetry is crucial for an array of cellular functions and plays an important role, for example, in membrane mechanical stability¹³ and the modulation of the activity of membrane proteins.¹⁴ Failure to maintain the asymmetric distribution of lipids can have dramatic consequences. For instance, the externalization of anionic phosphatidylserine lipids, which are normally localized in the inner leaflet of plasma membranes, is associated with cells undergoing programmed cell death¹⁵ and aids in the recognition and clearing of these cells from the healthy tissues of the organism.¹⁶

To maintain the asymmetric transmembrane lipid distribution, living cells employ special active mechanisms to selectively transport lipids across a membrane using specialized membrane proteins, flippases.^{17,18} Cells also use passive transport mechanisms that facilitate the migration of lipids from one leaflet to another, but these are as yet poorly understood. It is commonly assumed that the transbilayer movement of lipids is a single-molecule process,^{14,19} where the cooperative motion of neighboring lipids allows the flip-flopping lipid to more easily cross the transition state of the flip-flop event.^{20,21} Experimental data indicates that passive lipid translocation across a membrane is a pore-mediated process: It has been demonstrated⁵ that the experimentally determined activation energy for radioactive chloride flux across lipid membranes is close to the activation energy of lipid flip-flop.⁴ Furthermore, brief electric pulses (electroporation) have been shown to enhance the transbilayer mobility of phospholipids.²² All together, these findings suggest that a major fraction of passive lipid translocations takes place through water defects in membranes. Further examples of pore-mediated cellular processes include fusion events and maintenance of osmotic balance in cells.

The second major reason for the widespread interest in defect-mediated trafficking across cell membranes is in its relevance for numerous biomedical and biotechnological applications, such as drug and gene delivery into cells, cryopreservation, and others. A generic feature of drug delivery is the interaction of a drug molecule with specific membranes. To exert its pharmacological action, a drug molecule has to pass from an “external” to an “internal” site,

for example, from the gastrointestinal tract into the bloodstream. In doing so, a drug must cross a number of tissues and epithelia. Overcoming these barriers is one of the most important considerations in the drug delivery process. Consequently, there is considerable interest in developing physical and chemical means for enhancing the permeability of cell membranes to drug molecules. One of the possible ways to do so is to promote formation of transient defects spanning cell membranes, which in turn enhance unassisted transport of solutes through membranes. Experimentally, this can be achieved by the use of special chemical agents called penetration enhancers,²³ via application of an external electric field (electroporation)²⁴ or shock waves.²⁵ Furthermore, since passive lipid flip-flop is in most cases a pore-mediated process, poration of cell membranes could also be exploited to manipulate the lipid distribution across cell and organelle membranes.²⁶ This could give rise to an array of biomedical applications and possibly new therapeutic agents. Other related examples of defect-mediated processes in cell membranes include delivery of genes into cells with the use of nonviral synthetic vectors such as cationic lipids and dendrimers as well as antimicrobial peptides. Overall, manipulating the structure and properties of cell membranes in a controlled, and for specific applications in a reversible, manner is fundamental to numerous applications in the biosciences, pharmaceuticals, and biotechnology.

A dramatic increase in computer power and development of highly efficient simulation codes has recently made it possible to study a wide range of complex molecular systems at near-atomic resolution. For many biomolecular systems, the insight provided by computer modeling is unprecedented and invaluable: For instance, detailed molecular mechanisms of defect-mediated trafficking processes across cell membranes cannot be easily characterized experimentally, as they occur over molecular scales in roughly tens or hundreds of nanoseconds and are therefore beyond the resolution of most experimental techniques. Our paper aims to give a critical and a comprehensive review of major recent developments in the area of computer modeling of formation of transient membrane defects and related defect-mediated trafficking of solutes across biological membranes. The paper's focus is mostly on studies carried out in the past 5 year period. We only consider computational studies that employ molecular dynamics simulations at atomic (or near atomic) resolution. It is pertinent to emphasize that most of these studies required a substantial computer resource that has only become routinely available recently. The paper is organized as follows. We give a brief description of molecular dynamics simulations of lipid bilayers in section 2. Section 3 provides an overview of recent computational studies of formation of transient water defects (pores) in lipid membranes, with the poration being induced by a variety of factors, ranging from application of electric and mechanical fields to the effects of surfactants and lipid peroxidation. The next three sections are devoted to the defect-mediated transmembrane translocation of salt ions, lipid molecules, and polyelectrolytes such as DNA and cationic PAMAM dendrimers. We end with a short conclusion.

2. Molecular Dynamics Simulations of Lipid Bilayers

As biological membranes have a very complex structure and can contain hundreds of different lipid species and proteins, most experimental studies *in vitro* have focused

on simplified model systems such as lipid monolayers, planar lipid bilayers, supported bilayers, and multi- and unilamellar vesicles. Lipid aggregates such as bilayers in their biologically relevant, liquid-crystalline state are rather disordered structures. This prevents precise determination of the bilayer's structure at an atomic resolution using experimental methods such as diffraction. A viable alternative is computational modeling, which has now become an irreplaceable tool for studying models of biological membranes and often offers the only source of information as far as the membrane structure at atomic resolution is concerned. The methodology of molecular simulations of membrane systems has been discussed by Tieleman et al,²⁷ and the more recent development is discussed in recent papers together with the results. Here we discuss only the most central general themes related to simulations of membranes.

Computer modeling follows the same strategy as experimental studies in that it focuses on model membrane systems. In this paper we overview computational studies that employ molecular dynamics (MD) simulations to study biological membranes in atomic (or near-atomic) detail. Molecular dynamics is a simulation technique that treats a system in question as an ensemble of interacting sites (e.g., atoms). These sites or particles are assumed to obey classical mechanics, so that the evolution of a system with time is simulated through numerical integration of Newton's equations of motion for the particles. From the resulting MD trajectory, one can access various structural and dynamic properties of a system, including thermodynamic properties. We note that the family of Monte Carlo methods can serve as an alternative to MD simulation techniques, but their use for modeling biomembranes is limited, as Monte Carlo methods are not appropriate for generating nonequilibrium ensembles as well as for analysis of dynamical characteristics such as transport properties.

The interactions between particles in MD simulations are described through a force-field comprising a set of potential functions and associated specific parameters for the various atom types. Once a force-field has been set, all forces between interacting particles can be computed, provided that the positions of the particles are known. The primary focus of our review paper is on atomic-scale MD simulations; that is, we are interested in a situation when the interacting particles in a biomembrane system are explicit atoms rather than coarse-grained particles. This desire for high resolution dictates a rather small system size that can be handled using typical state-of-the-art computational resources. Therefore, most atomistic MD simulations are limited to small bilayer (or monolayer) patches of 100–1000 lipids with simulation times reaching hundreds of nanoseconds.^{27–30} The current state-of-the-art in atomistic simulations of membrane systems corresponds to scales of about a couple of microseconds with roughly 1 million atoms.^{31,32}

In the present article, only protein-free lipid membranes are considered. MD simulations of lipid bilayers with embedded membrane proteins constitute a separate area of research of considerable interest (several recent reviews^{33–35} are available in the literature).

As far as atomic-scale MD simulations of lipid bilayers are concerned, especially two force-fields are in common use: the all-atom CHARMM force-field^{36,37} and the force-field of Berger et al.,³⁸ which is a combination of GROMOS and OPLS force-fields. The main difference between them is in the fact that the CHARMM force-field explicitly

accounts for all the atoms in a bilayer system while the force-field of Berger et al. is a united-atom force-field; that is, nonpolar CH_2 groups of lipid acyl chains are treated as single particles. Both force-fields are calibrated empirically to reproduce available experimental data for lipid bilayers, such as, for example, the area per lipid, the deuterium order parameter of lipid tails, and the electron density profiles. Simulations with the pre-2010 versions of the CHARMM force-field were usually carried out in constant area ensembles due to subtleties arising in NpT studies;³⁹ these are resolved with the recently developed CHARMM36 parameter set,⁴⁰ and simulations can now be performed in the NpT ensemble. It is generally accepted that both of these atomistic lipid force-fields produce reasonably comparable results. The Berger force-field, being a united atom model, is somewhat less detailed but provides a gain in simulation performance due to reduction in the number of atoms compared to the all-atom CHARMM force-field.

In addition to the atomistic models, more coarse-grained models can also provide valuable information about the formation of transient defects in lipid bilayers. Therefore, we decided to include such simulation studies in the review as long as a coarse-grained model is sufficiently detailed to represent specific lipids, so that one can consider it as a model of near-atomic resolution. The force-field parameters of coarse-grained models are normally calibrated against available experimental data and data from related atomistic simulations. Due to the considerable reduction in the number of interacting sites, coarse-grained models can provide more than an order of magnitude gain over atomistic models. This makes it possible to study large-scale phenomena such as, for example, fusion of lipid vesicles. There are several coarse-grained models of lipid bilayers in the literature,^{41–43} of which the MARTINI model^{43–45} has been used in most studies relevant to the scope of this review. The parametrization of the MARTINI model is based on thermodynamic variables such as the solvation free energy, for which reason it is particularly appealing for large-scale studies.

In much of the early research effort, atomistic computational studies mostly dealt with single-component lipid bilayers. The majority of these studies were related to zwitterionic (uncharged) lipid bilayers,^{27–29} although simulations of anionic^{46–48} and even artificial cationic bilayers⁴⁹ were also reported. Later, more complex membrane models have emerged in an attempt to match the lipid composition of plasma membranes. One approach is to study many-component mixed lipid bilayers, of which the most relevant are ternary mixtures of phosphatidylcholine, sphingomyelin, and cholesterol.^{50–53} Such mixed bilayers are considered to be reasonable molecular models for the outer leaflets of cell membranes and have attracted much attention in the context of lipid rafts. Another more recent development is related to MD simulations of membranes with an asymmetric transmembrane distribution of lipid molecules typical of most living cells.^{54–58}

Despite the complexity that can be handled, most computational studies relevant to the defect-mediated trafficking across biological membranes have focused on single-component symmetrical lipid bilayers. A starting structure in these simulation studies is an unperturbed, pre-equilibrated lipid bilayer. As an illustration, we present a snapshot of such an unperturbed bilayer system comprised of 256 palmitoyl-oleoyl-phosphatidylcholine (POPC) lipids and ~10,000 water molecules in Figure 1. To induce formation

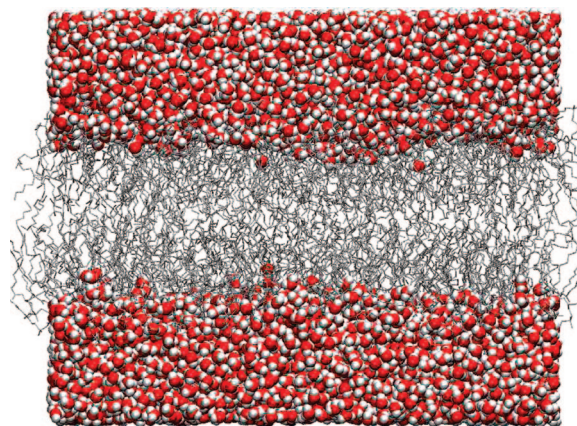


Figure 1. Unperturbed lipid bilayer system comprised of 256 palmitoyl-oleoyl-phosphatidylcholine (POPC) lipids and 10,249 water molecules. POPC lipid molecules are shown in gray and water in red-white.

of transient water defects in the bilayer, various factors such as external electric and mechanical forces, surfactants, antimicrobial peptides, and polyelectrolytes are then applied to the bilayer system.

3. Formation of Transient Defects in Lipid Membranes

3.1. Metastable Water Pores during Lipid Self-Assembly

Structural defects in membranes (such as, for example, water pores) imply changes with respect to the membrane's equilibrium state. Therefore, it is not surprising that the water pores were first observed in lipid aggregates far from equilibrium. In 2001 Marrink et al.⁵⁹ reported molecular dynamics (MD) simulations of spontaneous self-assembly of phospholipids into a bilayer structure. Starting from a random mixture of lipid molecules and water, the authors followed the entire process of the bilayer formation at atomic resolution. The initial steps in the lipid aggregation were found to be very fast, so that in just 3–5 ns one could witness the appearance of a bilayer whose structure, however, was not defect-free, as it contained a pore spanning the entire bilayer; see Figure 2. The pore turned out to be rather stable; its destabilization and disappearance, being the rate-limiting process in formation of an ideal bilayer, took, on average, about 15 ns but in some cases could last for up to 80 ns.⁵⁹ The hydrophilic pore observed during spontaneous self-assembly of lipids into a bilayer possessed several features typical of water pores induced in lipid membranes by other means: The pore of a nanometer diameter was stabilized by polar lipid headgroups and characterized by a fluctuating, toroidal shape;⁵⁹ see Figure 2.

Later, similar water pores were observed during spontaneous formation of a phosphatidylcholine vesicle in water.⁶⁰ Again, the initial self-organization of lipids in a vesicle-like structure was a rather fast process. However, the analysis of the resulting aggregate after 90 ns of MD simulations revealed that several water pores with diameters from 1 to 4 nm still remained in the vesicle. Due to high vesicle curvature, the pores seemed to be more stable than those in the case of planar bilayers.⁶⁰ The shape of the pores in the vesicle was found to be very similar to that observed in the study of self-assembled bilayers.⁵⁹ Furthermore, it turned out that the overall picture did not change much when a coarse-

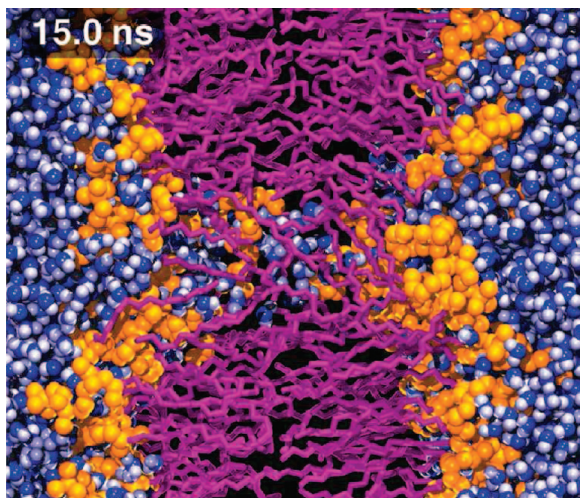


Figure 2. Metastable water pore observed for the first time at an atomic resolution during spontaneous aggregation of dipalmitoylphosphatidylcholine (DPPC) lipid molecules into a bilayer structure (shown is a system snapshot after 15 ns of simulations).⁵⁹ Headgroups and tails of DPPC lipids are shown in orange and purple, respectively; water is shown in blue. Reproduced with permission from ref 59. Copyright 2001 American Chemical Society.

grained model was employed to study vesicle formation.⁶¹ It should however be noted that, for the coarse-grained model, the water pores tend to be less stable compared to the atomistic counterpart due to a higher line tension.^{60,61}

3.2. Electroporation

Membrane electroporation is a widely used technique for permeabilization of cell membranes and skin through application of an external electric field. In general, one needs to distinguish two types of electroporation: conventional electroporation and supra-electroporation. The former involves rather long pulses (with duration from hundreds of microseconds to milliseconds) of low magnitude (0.1–1 kV/cm).²⁴ Supra-electroporation, being a relatively recent development, employs short (nanosecond-scale) electric pulses of large magnitude (up to several hundreds kV/cm).⁶² The principal difference between the two types of electroporation is in the fact that long, low magnitude pulses affect mostly the plasma membrane and are not felt by the interior of the cell. In contrast, supra-electroporation pulses go through the entire cell, so that electroporation of organelle membranes also becomes feasible.⁶³

Membrane electroporation is employed in numerous biomedical applications. It is routinely used to increase ionic and molecular transport across cell membranes in general and to transfer bioactive substances such as protein, DNA, and pharmaceutical compounds into the cell in particular. Ultrashort, high field electric pulses are used to promote phosphatidylserine externalization, apoptosis, and cancer cell killing. A basic hypothesis regarding the molecular mechanism of electroporation implies that an electric field induces the formation of transient hydrophilic pores in membranes.⁶⁴ However, until very recently, the exact molecular picture of the pore formation process remained obscure.

Following pioneering MD simulation studies by Tieleman et al.,^{65,66} membrane electroporation has attracted much attention among computational scientists. Atomic-scale molecular dynamics simulations are well suited for these

purposes, as they provide an unprecedented insight into the details of the electric field-induced pore formation.

To apply an electric field to the bilayer-water system in MD simulations, two different approaches have been employed. According to the first approach, an external electric field E was introduced in the system. The field E was applied perpendicular to the bilayer surface and was assumed to be uniform throughout the simulation box, so that a force $q_i E$ was added to all charged atoms in the system (here q_i is the charge of an atom).^{65–74} In most cases, the external electric field was set to be constant, although there were studies which employed a time-dependent external voltage.^{72,73} A constant electric field was also considered in the context of maintaining a nonzero membrane potential in MD simulations.⁷⁵ An alternative approach is to induce an electric field across a membrane through a transmembrane ionic charge imbalance.^{69,76–80} Such an imbalance is an inherent feature of most living cells; it is generally believed that it determines the resting membrane potential in cells, which is typically of the order of 100 mV. The local fluctuations in ion concentrations on the two sides of a membrane are at least in principle able to give rise to electroporation in cells, though they are expected to be rare processes. In simulations, it was demonstrated that the transmembrane ionic charge imbalance can successfully be used for pore formation, provided that the imbalance is sufficiently large (a 10–20-fold increase relative to the resting membrane potential is required).^{76,77} Here, we note that periodic boundary conditions employed in atomic-scale MD simulations of lipid bilayers prevent explicit modeling of the transmembrane ionic charge imbalance, as the periodic boundaries juxtapose the regions of high and low ionic concentration, canceling the potential across the bilayer. To overcome this, a double bilayer setup (i.e., two lipid bilayers in a simulation box) has been employed.^{81,82} This gives an independent control over the ionic composition of water regions on both sides of the membrane at an additional computational cost of simulating two bilayers (instead of one). Very recently, two alternative methods to model the transmembrane ionic charge imbalance have been proposed;^{83,84} both of them allowed one to avoid the use of a double bilayer setup. Tarek et al.⁸³ considered a lipid bilayer system in conjunction with the slab boundary conditions,^{85,86} which implied that the water baths on both sides of the bilayer terminated with a vacuum slab. This prevents ions from jumping across a simulation box without invoking a double bilayer setup. A drawback of the approach is that its use is restricted to the NVT simulations only.⁸⁵ Another limitation of the method is in the appearance of the surface tension at the water/vapor interface. Herrera and Pantano⁸⁴ have proposed an alternative approach which is also applicable to the NpT simulations: Instead of introducing vacuum slabs, the motion of ions is restricted in the direction perpendicular to the bilayer surface when the ions approach the edge of a simulation box, again thereby preventing jumps of ions across the box. This approach therefore breaks the periodic boundaries selectively just for the ions. Note that the ion-restraining potential introduces perturbations in the water phase, so that the water slab in the bilayer system should be increased accordingly to eliminate the effect of the perturbations on the water/lipid interface. Furthermore, the restraining potential slows down ion solvation as well as equilibration of ions within the lipid bilayer system.⁸⁴

Overall, an electric field applied to a lipid bilayer system can be quite different depending on the approach employed.

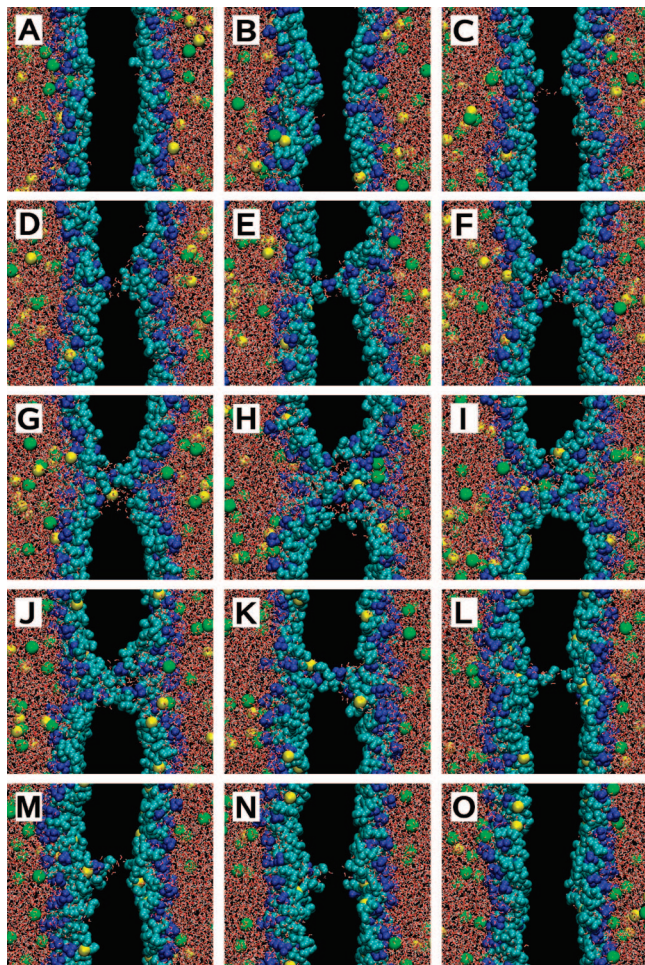


Figure 3. Dimyristoyl-phosphatidylcholine (DMPC) lipid membrane under electric field induced by a transmembrane ionic charge imbalance: Pore formation, ion transport, and membrane resealing. (A) 0 ns, (B) 1.1 ns, (C) 1.4 ns, (D) 1.45 ns, (E) 1.5 ns, (F) 1.6 ns, (G) 1.7 ns, (H) 2.5 ns, (I) 2.9 ns, (J) 4.5 ns, (K) 119.9 ns, (L) 122.1 ns, (M) 122.15 ns, (N) 122.2 ns, (O) 122.55 ns. Presented are the results for system 3 in ref 78 and the system pore6-NaCl_8 in ref 77. Choline groups of DMPC lipids are shown in blue, phosphate and glycerol groups of DMPC lipids in cyan, Na ions in yellow, Cl⁻ ions in green, and water in red-white. Nonpolar acyl chains of DMPC lipids are not shown. An excess of sodium ions is on the left-hand side.

Unlike in simulations with constant (or time-dependent) *external* electric field, a transmembrane ionic density gradient induces an electric field which is stochastic in nature: Such a field is determined by instantaneous positions of ions and is therefore subject to considerable fluctuations in time and space with respect to its average value. However, it turns out that the overall picture of the electric field-induced pore formation is not too sensitive to the particular details of the field. This can also be considered as a signature of the generic nature of the phenomenon observed. To illustrate membrane electroporation in more detail, we therefore chose to consider a bilayer system with a transmembrane ionic charge imbalance.

In Figure 3 we present formation of a water pore in a dimyristoyl-phosphatidylcholine (DMPC) lipid membrane. A transmembrane charge imbalance of Na⁺ ions induces on average a voltage of ~ 2.12 V across the membrane (corresponding to a field of ~ 0.30 V/nm).^{77,78} Under this field one can witness noticeable perturbation of the water/lipid interface accompanied by rather deep penetration of some of water molecules into the interface (Figure 3B). After ~ 1.4

ns of simulation, one can see the appearance of a single water defect spanning the entire membrane (Figure 3C). This file of water molecules was recently identified as an intermediate pore state.⁷⁴ We note that the formation of a single water defect is not necessarily followed by formation of a stable pore.⁶⁶ In this particular system, the single water defect grows rapidly, leading to a considerable redistribution of lipid headgroups from the water–lipid interface to the membrane interior; see Figure 3D–H. The polar lipid headgroups surround and stabilize the pore; it was recently demonstrated that one could observe a field-driven alignment of the headgroup dipoles which formed the pore walls.⁷⁰ The entire pore formation process—from appearance of a single water defect to a stable pore—takes on average around 1 ns.

The equilibrium size of a stable pore was studied in ref 74, where, in agreement with experimental data,^{87,88} the average pore radius of ~ 0.5 nm was reported. Similar pore radii (ranging from 0.4 to 1.1 nm) were observed in ref 77. A stable pore was shown to be lined with around 8–10 lipid headgroups.^{74,77} In contrast, Tieleman reported formation of much larger electropores (up to 10 nm in diameter) in a very large lipid bilayer patch comprising 2300 lipids.⁶⁶ It was argued⁷⁴ that such large pores are likely caused by an artificially enhanced electric field in the pore region due to periodic boundary conditions and the particle-mesh Ewald (PME) method used to handle electrostatic interactions. Furthermore, the deformation of a simulation box upon field-induced deformation and folding of a bilayer can have an amplifying effect: The total potential difference across the box increases considerably when the bilayer folds double (Tieleman, private communication). It should be kept in mind, however, that irreversible breakdown due to electric fields is a real phenomenon and is observed experimentally when a high enough field is applied to the membrane for a sufficiently long time.⁸⁹

In addition to pore formation, membrane resealing after the electric field is switched off is an important consideration, as it directly relates to the problem of reversibility of changes in cell membranes caused by electroporation. The membrane resealing was studied in ref 67, where a complete reconstruction of a lipid bilayer with a pore was witnessed within just a few nanoseconds after switching the transmembrane voltage off. However, it turns out that the way the electric field is switched off matters. For instance, if an external electric field is not turned off completely but strongly reduced instead (from 0.5 to 0.04 V/nm), an electropore can stay stable for tens of nanoseconds.⁷⁴ Furthermore, in the computational studies where an ionic charge imbalance was employed, the discharge of the transmembrane voltage was essentially gradual due to the pore-mediated ion leakage. In this case, after the voltage was nearly (but not necessarily fully) discharged, the water pore became metastable and could stay open for more than 200 ns.^{76–79} An illustration of this process is shown in Figure 3: After 4.5 ns, when leakage of most ions has finished, the electropore stays open for almost 115 ns; see Figure 3J and K. However, at some point the size of the pore becomes smaller than a certain threshold and one can observe the pore closure which occurs on a nanosecond time scale; see Figure 3K–O.

Ziegler and Vernier recently performed a series of MD simulations aiming to establish as to how the strength of the porating field is linked with the length of lipid acyl chains in a bilayer.⁷¹ They found that the minimum porating field depends strongly on the thickness of a bilayer: Thinner

bilayers require weaker fields for pore formation. However, the absolute values of the threshold porating fields reported in ref 71 should not be taken as definitive, as they are dependent on the size of the bilayer system studied and on the length of simulations. In particular, smaller bilayers are more difficult to electroporate due to suppressed undulations. Furthermore, the simulation time span considered (25 ns in ref 71) might not be statistically long enough. It seems that a threshold field value also depends on the way the electric field is applied, namely a transmembrane ionic charge imbalance tends to give lower threshold fields. For instance, the minimal value of the porating electric field due to a transmembrane imbalance of potassium ions was found to be 0.23 V/nm for a DMPC bilayer.⁷⁷ The corresponding limiting value of an *external* field for thinner dilauroyl-phosphatidylcholine (DLPC) bilayers was in turn reported⁷¹ to be 0.26 V/nm. It should however be kept in mind that state-of-the-art atomic-scale molecular dynamics simulations are not able yet to provide us with definitive conclusions regarding threshold fields. In addition, it was demonstrated that the presence of a peptide nanotube channel⁶⁷ or a polypeptide antibiotic gramicidin A⁹⁰ in a bilayer suppresses electroporation. The same effect is also to be expected for cholesterol,⁹¹ though cholesterol-induced effects for phenomena related to electroporation can also depend on the concentration of cholesterol.⁹²

In general, the electric fields employed in the computational studies are considerably larger than those used in electroporation experiments. This is due to obvious limitations regarding the system size and the time scales accessible in state-of-the-art atomic-scale MD simulations. To increase the probability of the pore formation, one needs to lower the energy barrier for the pore formation by increasing the electric field strength. In this regard, supra-electroporation experiments which employ nanosecond-long strong electric pulses are very attractive in the context of comparison with simulation data. In particular, in a recent supra-electroporation study by Frey et al.⁶² the peak value of 1.6 V was reported for the voltage across the membrane. This value is close to the threshold porating voltage of 1.64 V observed in MD simulations of electroporation of DMPC lipid bilayers.⁷⁷

Atomic-scale molecular dynamics simulation studies are able to shed light not only on the molecular details of the pore formation process but also on its driving force. According to Tieleman,⁶⁶ pore formation is driven by local electric field gradients at the water/lipid interface. These electric field gradients are thought to interact with water dipoles, increase the probability of formation of water defects in the membrane interior, and also stabilize existing defects. The latter was nicely illustrated in recent MD simulations of oxidized lipid bilayers:⁹³ As incorporating oxidized lipids into lipid membranes was shown to promote formation of water defects⁹⁴ (see section 3.8 for more details), electroporation of the membranes was also facilitated considerably by oxidative damage.

Rather surprisingly, a dipolar nature of lipid headgroups plays a negligible role in the initial steps of pore formation: while early stages of the pore formation involve some reorientation of lipid headgroups,^{70,74} electroporation has also been observed in a water/octane system which lacks polar headgroups.⁶⁶ Therefore, it appears that the water dipoles are crucial for electroporation. One of the implications is that coarse-grained models are probably unsuitable to study

this kind of phenomenon as long as they do not preserve the dipolar structure of water molecules (we recall that, for example, the MARTINI coarse-grained model^{43,44} treats four water molecules as a single particle). Indeed, all the reported simulation studies of electroporation have explicitly included water molecules.

Comparison of the results of *in silico* modeling with experimental electroporation studies is a difficult and non-trivial task due to the time and scale limitations inherent for atomistic computational models and the nature of boundary conditions and algorithms used to handle electrostatic interactions in simulations. In addition to the above-mentioned necessity to employ short electric impulses of large magnitude in simulations, one can also mention the limitations related to the size of a bilayer patch accessible in atomic-scale MD simulations: A standard lipid bilayer system is characterized by a lateral size of around 5 nm × 5 nm (which is then extrapolated by periodic boundaries), so that formation of just a single electropore is observed in most cases. This, in particular, means that the equilibrium pore density is not accessible from atomic-scale MD simulations of lipid bilayers. The only direct comparison of simulation results with experimental data was carried out in a recent study by Böckmann et al.,⁷⁴ who linked the (single event) preparation times measured in simulations with macroscopic prepore formation kinetics seen in experiments.

Given the challenge of interpreting membrane-level MD simulations of electroporation phenomena in terms of experimental studies, combined use of atomistic simulations and cell-level analytical and numerical models^{63,95–100} will be of tremendous importance in the future. These two levels of description, molecular and cellular, are complementary and would benefit by being considered together. In particular, redistribution of voltage over the plasma membrane of a cell should be consistent with pore formation and pore-mediated transport at the membrane level. It is therefore important to use membrane-level insight gained from atomic-scale MD simulations to generate better cell level models and vice versa.

3.3. Tension-Induced Pores

Hydrophilic water pores can also be induced in protein-free lipid membranes by applying mechanical stress, with pipet aspiration experiments^{101–103} being a well-known example of this type of technique. On the computational side, the pore formation due to applied surface tension has been addressed in a series of studies by Marrink et al.^{43,65,104–106} In general, as far as the intact lipid membranes are concerned, membrane rupture under mechanical stress is known to depend strongly on the rate at which the stress is applied.¹⁰⁷ The time scales over which lipid membranes porate and rupture at low loading rates are currently not accessible from atomic-scale molecular dynamics simulations. Spontaneous pore formation can be observed in simulations only when the applied tension is very large. Taken together with the fact that the tension is applied to the bilayer system almost instantly, this can be interpreted as the regime of high loading rates. In particular, Marrink et al.^{65,104} showed that surface tension as high as 90 mN/m needs to be applied to an intact DPPC bilayer to induce the formation of a pore. The pore formation process starts with the penetration of water molecules toward the bilayer interior. When the “water fingers” meet in the middle of a bilayer, a complete water channel is created which grows then very rapidly. Almost immediately

(just within 2 ns) after the pore has been formed, the lipid bilayer gets disrupted.^{65,104} The latter is in line with the kinetic nature of the process: At high loading rates, the formation of the pore itself is the rate-limiting event.¹⁰⁷ We also note that the threshold tension in the rupture simulations could depend on the system size; namely, one can expect a decrease of the critical tension with the size of a bilayer patch.¹⁰⁸

Apart from studying intact lipid membranes under mechanical stress, the membranes with preformed hydrophilic pores have also been considered.¹⁰⁴ Such pores could be formed, for example, during the process of aggregation of lipids from random solution into a bilayer structure.⁵⁹ It turns out that the applied surface tension is able to stabilize a water pore which otherwise gets closed within a 100 ns time span under stress-free conditions.¹⁰⁴ The size of a stable pore lined with lipid headgroups increases with the magnitude of the applied tension, with the minimum pore radius observed being 0.7 nm. What is more, there exists a certain threshold surface tension (~ 38 mN/m)¹⁰⁴ beyond which a bilayer with a preformed pore becomes very unstable: The pore expands, and the bilayer gets destroyed. Interestingly, these findings are in line with several theoretical models which are based on the idea that for small hydrophilic pores the free energy of pore formation has two main contributions: the line tension that opposes pore formation and the surface tension that favors creation and expansion of the pore¹⁰⁹ (see also section 3.9). Therefore, depending on the magnitude of the surface tension, one can expect either stabilizing or destroying metastable water pores in membranes. It should be noted that the absolute value of the critical surface tension at which a hydrophilic pore can be stabilized is sensitive to the simulation details, namely to the way in which the electrostatic interactions are handled. While the straight cutoff simulations give 38 mN/m for the limiting tension,¹⁰⁴ the use of the reaction field method¹⁰⁴ and the particle-mesh-Ewald (PME) technique¹⁰⁶ for the electrostatics reduces this value to 18 and 15 mN/m, respectively. Given that both reaction field and PME methods provide limiting tension values which are closer to the experimental ones, this could be one more argument to avoid the straight cutoff of the electrostatic interactions in lipid bilayer simulations.^{110–112}

The effect of salt ions on the stability of water pores has been studied in ref 106. It turns out that NaCl salt is able to destabilize a hydrophilic pore so that one needs to apply higher surface tension to stabilize the pore as compared to a salt-free situation. The effect is found to be concentration-dependent; that is, higher NaCl concentrations lead to shorter lifetimes of pores under stress-free conditions. The overall effect of NaCl salt was linked to the well-known binding of sodium ions to the polar headgroups of the lipids^{82,113–115} which line the walls of a hydrophilic pore: This way ions significantly increase the pore line tension, so that higher surface tension is required to stabilize the pore. For instance, adding 0.2 M of NaCl salt gives rise to a 2-fold increase in the line tension.¹⁰⁶ Generally speaking, similar effects can also be expected for other biologically relevant cations, with the effect being strongly dependent on the ability of ions to adsorb onto the lipid/water interface of zwitterionic lipid membranes. Therefore, one can anticipate strong destabilizing ability for divalent Ca^{2+} ions,¹¹⁶ while K^+ ions will destabilize hydrophilic pores to a significantly lesser extent than Na^+ ions.¹¹⁵

The tension-induced pore formation has also been studied with the use of coarse-grained models.⁴³ In contrast to

simulations of electroporation phenomena, the results found for the models of lower resolution turned out to be quite close to those gained through atomic-scale simulations: Since pore formation here is due to mechanical stress applied to the membrane rather than electric field induced reorientation of water dipoles, the dipolar nature of water molecules is not crucial for tension-induced pore formation. The pores observed in coarse-grained simulations⁴³ were similar in shape, and preexisting pores could be stabilized at a critical tension of 25 mN/m. The average radius of tension-stabilized pores was estimated to be in the range from 1.5 to 2.0 nm,⁴³ which is larger than that reported in atomic-scale simulations ($r = 0.9$ nm).¹⁰⁴ The line tension was also found to be larger for pores observed in coarse-grained simulations:⁴³ 5×10^{-11} N versus $(1.5 - 3) \times 10^{-11}$ N estimated via atomic-scale simulations.^{104,106} Given that experiments^{101,107} reported the value of $\sim 1 \times 10^{-11}$ N, one can conclude that the properties of pores observed in atomic-scale simulations are somewhat closer to those observed in experiments. As for the intact lipid bilayers, a pore was formed within nanoseconds when a tension of 100 mN/m was applied⁴³ (cf. with 90 mN/m reported for atomistic models).^{65,104} In turn, when tension was reduced to 65 mN/m, several microseconds were required for a pore to be formed.⁴³

Apart from the bilayers, the formation of water pores in lipid monolayers has also been studied.¹⁰⁵ In simulations of monolayers, a surface tension can be applied simply by increasing the area of a monolayer. Knecht et al.¹⁰⁵ reported formation of transient holes in a DPPC monolayer when the area per lipid was as large as 0.98 nm². At even larger areas (~ 1.05 nm²/lipid) the monolayer ruptures and a stable pore is formed. The authors therefore concluded that at this area the monolayer system entered into the liquid–gas coexistence phase.¹⁰⁵

3.4. Water Pores Induced by Shock Waves

Another cell permeabilization technique involves the application of shock waves, i.e. high pressure waves which propagate at a supersonic speed and pass the cell membranes within a very short time (several picoseconds).^{117,118} Several studies have suggested that shock waves could induce formation of transient pores (so-called sonoporation); the pores serve as pathways for solute permeation across a membrane.^{25,119,120} The effect of shock waves on lipid bilayers was addressed by Koshiyama et al.^{121–123} with the use of nonequilibrium atomic-scale MD simulations. Technically, the effect of shock waves on a bilayer system was modeled through the increase of momentum of water molecules. The authors demonstrated that action of shock waves on a lipid bilayer consists of two stages—the collapse and the rebound stages—and that the lipid bilayer undergoes considerable structural changes, such as bilayer thinning and disordering of lipid chains. Essentially, this was accompanied by penetration of a significant amount of water molecules into the hydrophobic core of a bilayer.^{121–123} Note that due to periodic boundary conditions the simulations need to be terminated at the moment the effect of a shock impulse reaches the opposite side of a simulation box. Therefore, the simulations had to be very short (up to 1 ps) despite the relatively thick water layer used in simulations (~ 14 nm).¹²¹ The limited simulation time scales prohibited the study of dynamics of water molecules which permeated into the bilayer due to shock waves. To address this problem, Koshiyama et al.¹²² performed a series of equilibrium MD

simulations of lipid bilayers in whose interior a certain amount of water molecules was preinserted. It turned out that when the number of water molecules in the bilayer interior was large enough (more than 1000 H₂O inside a bilayer of 128 lipids), one could witness clustering of water molecules inside the membrane with subsequent formation of a hydrophilic pore.¹²² The water pore was found to have an hourglass shape, of about 1.9 nm in diameter, and stayed open for more than 35 ns. It was therefore suggested that shock waves could porate cell membranes. However, accurate modeling of the entire process—from shock wave application to formation of transient water pores in a membrane—is still an open issue.

3.5. Membrane Defects Induced by Surface-Active Molecules

Amphiphilic molecules or surface-active molecules constitute a wide class of compounds whose chemical structures are characterized by the existence of covalently linked hydrophilic and hydrophobic groups. Such molecules are soluble in both polar and organic solvents. In fact, lipid molecules themselves are amphiphilic, so that the hydrophobic interaction plays a major role in their ability to organize into a bilayer structure. Therefore, one can expect that surface-active molecules should interact strongly with the lipid membranes given that they can get incorporated into the bilayer structure, hiding their hydrophobic parts in the membrane interior. Thus, such amphiphilic molecules can potentially be employed for controlled modulation of the structure and properties of cell membranes, which is fundamental to numerous applications in bioscience, pharmaceuticals, and biotechnology.

A fascinating small molecule with an amphiphilic character is dimethylsulfoxide (DMSO), which comprises a hydrophilic sulfoxide group and two hydrophobic methyl groups. DMSO is widely employed in cell biology as an effective penetration enhancer,²³ a cryoprotectant,¹²⁴ and a cell fusogen.¹²⁵ Interestingly, DMSO is able to promote permeation of both hydrophobic¹²⁶ and hydrophilic¹²⁷ species across cell membranes, the latter is difficult to explain without making an assumption that DMSO induces formation of water pores which serve as pathways for transport of hydrophilic molecules.

To reveal the molecular mechanism of action of DMSO on lipid membranes, atomic-scale¹²⁸ complemented with coarse-grained¹²⁹ MD simulations of lipid/water/DMSO systems have been carried out. In the comprehensive atomistic simulations,¹²⁸ the DMSO concentration was systematically varied from 0 mol % (pure water) to 100 mol % (pure DMSO solvent). It was found that the modes of DMSO action are concentration-dependent and there exists a certain range of concentrations (from 10 to 20 mol % in ref 128) in which DMSO indeed induces formation of hydrophilic water pores in a phospholipid membrane.

In general, DMSO molecules are found^{128,129} to readily penetrate into the lipid/water interface; this is accompanied by the loss of lateral interactions between the lipid headgroups of different lipids, by the bilayer expansion,¹³⁰ and by the related drop in the bilayer thickness. As a result, the lipid/water interface becomes rather prone to structural defects due to, for example, thermal fluctuations, which can result (within a certain DMSO concentration range) in pore formation.¹²⁸

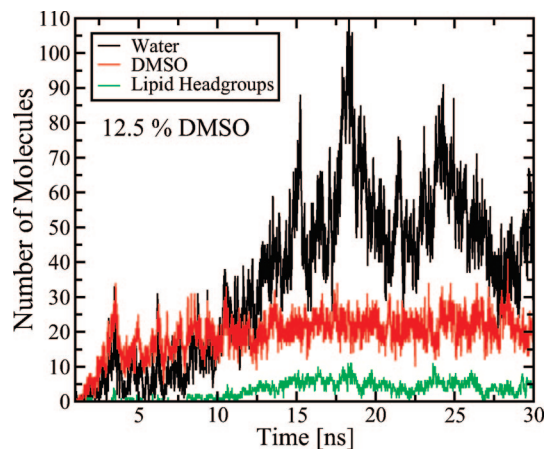


Figure 4. Time evolution of the number of water molecules (black), DMSO molecules (red), and lipid headgroups (green) within a 0.5 nm slab in the middle of a DPPC membrane during the pore formation in the bilayer system with 12.5 mol % of DMSO. Adapted with permission from ref 128. Copyright 2007 American Chemical Society.

The dynamics of the DMSO-induced pore formation is illustrated in Figure 4 for a DPPC lipid bilayer in aqueous solution with 12.5 mol % of DMSO (lipid-free basis): First, DMSO molecules partition into the membrane interior; then water enters into the membrane via DMSO-mediated structural defects. Finally, because of thermal fluctuations, the amount of water molecules within the membrane can become so large that a significant reorientation of lipid headgroups toward the membrane interior is required to minimize the free-energy of the system. This completes the formation of a hydrophilic pore spanning the membrane.¹²⁸ We note that the molecular mechanism of the DMSO-induced membrane poration seems to be of a generic nature and is not sensitive to the computational model employed: Similar DMSO action was observed in both atomistic and coarse-grained simulations.^{128,129} Further increase in DMSO concentration makes the water pores larger in size and promotes formation of multiple pores. Eventually, this leads to a complete disintegration of the bilayer structure of a lipid membrane (for concentrations higher than 20 mol %).¹²⁸

Another small molecule with surface active properties is alcohol, especially ethanol, which is the most widely used alcohol. Ethanol is the active component of alcoholic beverages; it also has applications as a food preservative, as a permeability enhancer in transdermal drug delivery, and as a model anesthetic. There are numerous experimental indications that the amphiphilic nature of ethanol allows the structural and mechanical properties of lipid membranes to be changed through partitioning of ethanol into the membrane. As ethanol is a short-chain alcohol and its hydrophobicity is rather limited, after partitioning, ethanol molecules are primarily located within the water/lipid interface, forming hydrogen bonds with hydrophilic lipid headgroups.^{131,132} Overall, ethanol has a disordering effect on lipid hydrocarbon tails, giving rise to the increase in the fluidity of the membrane^{133,134} which is accompanied by a reduction in the membrane rigidity.^{135,136}

Most of these experimental findings have been confirmed by atomic-scale MD simulations^{132,137–142} that have focused mostly on relatively low ethanol concentrations. Only very recently the simulation studies were extended to high concentrations of ethanol (up to 30 mol %).¹⁴³ It was observed that when the ethanol concentration increases

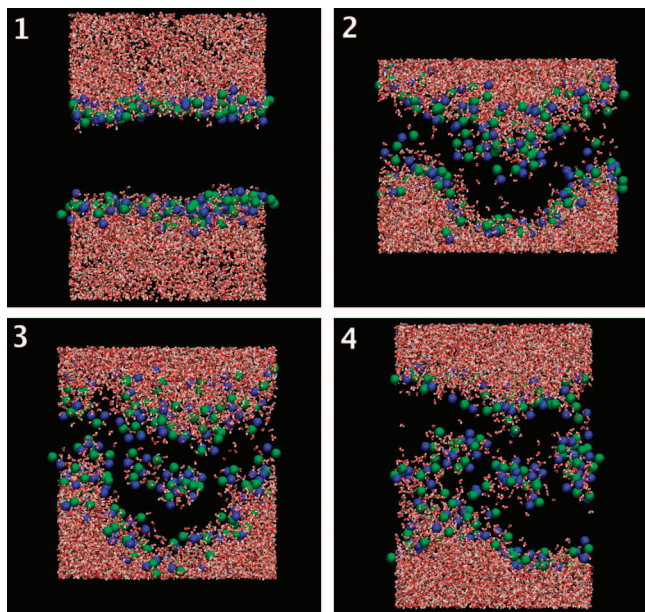


Figure 5. Formation of nonbilayer micelle-like structures within the membrane interior for a POPC system with 15 mol % of ethanol: (1) 3,100 ps; (2) 13,180 ps; (3) 19,920 ps; (4) 30,000 ps. Shown are water molecules (red and white) and phosphorus (green) and nitrogen (blue) atoms of lipid headgroups. The rest of the lipid atoms as well as ethanol molecules are not shown. Reproduced with permission from ref 143. Copyright 2009 American Chemical Society.

beyond a certain threshold level (12 mol % or 30.5 v/v %), the character of the ethanol-induced changes in a bilayer system becomes different from what is observed at low and moderate concentrations; see Figure 5. The progressive thinning of a membrane due to accumulation of ethanol molecules makes the lipid/water interface unstable and prone to formation of defects, so that one can witness desorption of water clusters surrounded by lipid headgroups toward the membrane interior. As a result, the bilayer structure of a lipid membrane becomes partly destroyed.¹⁴³ One has several nonbilayer globular structures in the membrane interior, which have the form of irregular “inverse micelles”; see Figure 5. The micelle formation in the membrane interior appears to be generic, being reproducible in the simulations of both palmitoyl-oleoyl-phosphatidylcholine (POPC) and palmitoyl-oleoyl-phosphatidylethanolamine (POPE) lipid bilayers with ethanol. Interestingly, formation of a water pore spanning the entire membrane does not occur in lipid bilayers under the influence of ethanol, in contrast to the situation observed in the simulations of lipid/water/DMSO systems. This difference might be due to strong hydrogen bonding interaction between ethanol molecules and the lipid headgroups. These interactions, being absent in the case of DMSO (DMSO is a H-bond acceptor only, while ethanol participates as both a H-bond acceptor and donor), can considerably reduce headgroup hydrophilicity and effectively screen the lipid headgroups from their counterparts in the opposite leaflet, leading to the formation of the micelle-like defects rather than water pores.¹⁴³ Formation of the micellar structures clearly involves desorption of lipids, suggesting that ethanol reduces the lipid–lipid interaction. In contrast, with DMSO the membrane (while being very flexible) appears to be more robust in retaining contiguity, and hence preferring formation of a pore over lipid desorption.

Remarkably, these computational results show good agreement with experimental data. It has been observed experi-

mentally that at high ethanol concentrations (exceeding 29.4 v/v %) the bilayer structure of DPPC membranes could not be maintained, so that formation of small globular structures was observed.¹⁴⁴ On the other hand, Isomaa et al.¹⁴⁵ have demonstrated that small amphiphilic molecules are able to alter the shape of membranes of human erythrocytes through the formation of the nonbilayer phases within the membrane interior, thereby protecting the erythrocyte membrane against collapse. Furthermore, similar lipid micelle-like structures in the presence of a high concentration of ethanol have also been reported upon formation of sponge mesoporous silica materials with phospholipid bilayers used as a template.¹⁴⁶

Given the notable impact of a short-chain alcohol such as ethanol on lipid membranes, one can expect that the effect of related alcohol molecules with longer chains should be stronger and be witnessed at smaller concentrations compared to the case of ethanol. Indeed, the longer the alcohol’s hydrocarbon chain, the lower its solubility in water and correspondingly the more easily it should be for it to partition into the membrane interior. Longer hydrocarbon chains also imply larger defects in the lipid/water interface due to alcohol. This has clearly been demonstrated in a MD simulation study¹⁴⁰ of phospholipid membranes in aqueous solution with ethanol, propanol, and butanol. In particular, butanol at a concentration of just around 1 mol % is able to develop considerable defects in the membrane structure: Butanol molecules move rather freely inside the membrane from one leaflet to another. The gaps in the interface due to such butanol movements are found to be large enough to serve as a pathway for lipid translocations,¹⁴⁰ see also section 5.2.

As for the other types of long-chain surface-active molecules, a nice illustration is given in a computational study of the effects of resorcinolic lipids on phospholipid bilayers.¹⁴⁷ Alkyl-resorcinolic lipids or resorcinols are a class of compounds occurring mostly in the membranes of higher plants; they have attracted much attention in agriculture and medicine due to their biological activity. Resorcinols are amphiphilic molecules with a single hydrocarbon chain as the hydrophobic tail and a dihydroxybenzene ring as the polar head. Marrink et al.¹⁴⁷ studied the effect of resorcinols solvated in the water phase on phospholipid bilayers. Three homologues which differ in the tail length (11, 19, and 25 carbon atoms) were considered. Prior to interaction with the lipid bilayer, the resorcinols which are randomly distributed in water were found to rapidly aggregate in a micellar structure, with the aggregation process taking just several nanoseconds. The resulting micelle is then bound to one of the leaflets of the lipid bilayer. The simulations show that this is a critical moment which defines the overall effect of resorcinols on the bilayer.¹⁴⁷ If the micelle formed by resorcinols remains compact, one can observe a strong deformation of the bilayer: The micelle forces phospholipids from the closest leaflet to the bilayer center, the structure of the leaflet is disrupted, and phospholipids start to surround the micelle. This eventually results in the formation of a water pore which either gets closed or leads to rupture of the bilayer with the formation of the nonlamellar hexagonal phase structure.¹⁴⁷ If the micelle lost its integrity upon binding to the bilayer, the resorcinols form a layer on the bilayer surface and no pore formation is observed. Furthermore, of remarkable interest is the fact that if resorcinols are preincorporated into the bilayer, their presence leads to stabilization of a membrane rather than inducing the structural defect

described above: The membrane becomes thicker and less permeable to water. These findings highlight a dual effect which resorcinolic lipids exert on phospholipid membranes.¹⁴⁷

The effect of inclusions of rather long-chain surface-active molecules into lipid bilayers was recently studied by Marrink et al.¹⁴⁸ They considered DPPC bilayers with inclusions of dioctanoyl-phosphatidylcholine (diC₈PC) molecules which were inserted asymmetrically into one of the leaflets of a bilayer. The asymmetric insertion of foreign molecules induces stress due to expansion of one of the leaflets with respect to its diC₈PC-free counterpart, leading to the bilayer instability. Furthermore, cone-shaped diC₈PC molecules do not pack well with cylindrically shaped DPPC lipids in a planar bilayer and are expected to destabilize the bilayer through formation of positively curved structures such as pores. As a result, one can expect that the stress accumulated in asymmetric DPPC-diC₈PC/DPPC bilayers could be released through the formation of transmembrane water pores, with subsequent pore-mediated transport of DPPC and diC₈PC molecules from the overpopulated to the underpopulated leaflet. As demonstrated in ref 148, this is indeed the case, provided that the asymmetry (DPPC-diC₈PC/DPPC) ratio is sufficiently large (namely, larger than 64/34). The finding also highlights the importance of the molecular shape of inclusions for their ability to permeabilize the membrane: When cylindrically shaped DPPC molecules were used as inclusions, no pore formation was observed for any asymmetry ratios.¹⁴⁸

3.6. Peptide-Induced Poration of Membranes

Small cationic peptides are known to induce considerable distortions in the membrane structure which often result in pore formation. This section discusses two major families of such peptides: antimicrobial peptides and cell-penetrating peptides.

Antimicrobial peptides (AMP) are short amphiphatic peptides which carry a net positive charge under physiological conditions.¹⁴⁹ The peptides, being an integral part of the immune system of higher organisms, show a wide range of antimicrobial activity. Much recent interest in AMP has been triggered by the increasing resistance of bacteria against conventional antibiotics. From this perspective, a thorough understanding of the molecular mechanism of AMP action on membranes is highly desirable.

Most AMP are believed to induce the direct lysis of the target bacterial membrane.¹⁵⁰ Recent advances in computer power and methodology have made it possible to follow the entire process of the AMP mode of action—from initial binding of a peptide to poration—in atomistic detail. In particular, a landmark study by Marrink et al.¹⁵¹ has focused on the magainin MG-H2 peptide interacting with a model phospholipid membrane. This positively charged peptide (+3) is well characterized experimentally; at high concentration it is able to permeabilize membranes^{152,153} via forming hydrophilic nanosized pores, eventually triggering cell death.

The setup of the simulations by Marrink et al.¹⁵¹ mimics the experimental situation when peptides are added to solution containing cells or liposomes: Magainin molecules are initially placed in the water phase asymmetrically with respect to the membrane, so that they are able to adsorb to one leaflet only. The authors showed that above a certain threshold concentration the peptides induce the formation of pores in the membrane.¹⁵¹ This process was found to be

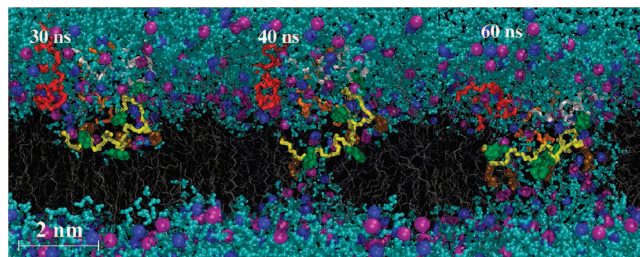


Figure 6. Spontaneous pore formation in a DPPC lipid bilayer induced by the antimicrobial magainin peptide MG-H2. Presented are snapshots at 30, 40, and 60 ns. The backbones of the different peptides are shown in yellow, orange, red, and white. The lipid tails are gray, water is cyan, and the headgroups are shown as blue (choline) and purple (phosphate) spheres. Adapted with permission from ref 151. Copyright 2006 American Chemical Society.

cooperative; that is, to trigger the formation of pores, the peptides need to aggregate.

Figure 6 shows the essential steps in the magainin-induced pore formation when four copies of peptides are placed in solution near the surface of a bilayer comprised of 128 lipids (the corresponding peptide/lipid ratio is 1/32). Magainin molecules that are distributed randomly in the aqueous phase bind to the lipid/water interface within 10 ns. Upon binding, the peptide molecules aggregate. Furthermore, they orient in such a way that their hydrophobic side chains interact with the interior of the membrane. Then, one of the magainin molecules begins to embed deeper into the membrane; see the snapshot at $t = 30$ ns in Figure 6. The embedding of the peptide, together with the fact that its charged lysine residues remain hydrogen bonded with the lipid headgroups of the leaflet to which peptides are bound, leads to increased fluctuations in the lipid/water interface. These fluctuations eventually trigger the interactions of the hydrophilic groups of the embedded peptide with water molecules from the opposite, peptide-free interface; see the central snapshot in Figure 6. Once solvent molecules make contact with the embedded peptide, a hydrophilic pore opens within a few nanoseconds, as seen in the right-hand-side snapshot of Figure 6. The resulting pore was found to be stable and demonstrated slow relaxation toward a toroidal shape.

It is instructive to note that binding of magainin peptides to the membrane creates a local tension. Since the peptides bind to one leaflet only, the resulting tension is asymmetric with respect to the two monolayers.¹⁵¹ It is of compressive nature for the leaflet to which the peptides are bound, while the opposite, peptide-free leaflet expands. Interestingly, application of an external stress was found not to speed up pore formation, indicating that only the difference in stress between the two leaflets matters.¹⁵¹

One of the most important findings of the study¹⁵¹ was the observation that the shape of the magainin-induced pore differs significantly from that of the conventional toroidal pore. The peptides that form the pore are largely disordered and can adopt various orientations. Only one or two peptides are located near the center of the pore. The rest remains bound at the membrane surface close to the rim of the pore. To distinguish the irregular pores observed in simulations from idealized toroidal pores, the authors introduced the term disordered toroidal pore (DTP) model.¹⁵¹

Two other computational studies^{154,155} have demonstrated that the proposed DTP model is most likely of generic nature. The studies have focused on two cationic AMPs of different secondary structure in the membrane environment: melittin¹⁵⁴ and cateslytin.¹⁵⁵ The former is known to form preferably

an α -helical structure when bound to the membrane (similar to magainin H2). In contrast, the latter adopts a β -sheet structure. Both studies found that the main steps in the AMP-induced poration are very similar to those observed previously for magainin; the shape of the transmembrane pores were found to resemble the DTP model proposed by Marrink et al.¹⁵¹ Thus, one can conclude that the secondary structure of an AMP does not have a significant impact on its ability to form pores. The prerequisites for pore formation appear to be a rather high concentration of AMPs in solution (higher than a certain threshold peptide/lipid ratio) and aggregation of peptides.

The important implication of these findings is that a net electric charge of peptide aggregates is a key factor which drives formation of water pores in membranes. In most cases, a large enough charge has to accumulate *asymmetrically* nearby the membrane interface for initiating pore formation. Such a charge induces the local electric field across the membrane, making the situation reminiscent of electroporation (so-called molecular electroporation).^{76,156,157} Indeed, as demonstrated in ref 155, adding 8 cateslytin peptides (with +5 charge each) in the aqueous solution close to one side of a membrane of 128 lipid molecules creates a roughly constant electric field (~ 0.1 V/nm) in the hydrophobic core of the membrane. Therefore, the electrostatic effect of cationic molecules on a lipid membrane is similar in a way to the action of an external electric field. Furthermore, it turns out that application of an additional electric field to a membrane-AMP system considerably speeds up formation of the AMP-induced pores,¹⁵⁵ most likely because the external field promotes deeper embedding of the peptides into the membrane. The importance of charges in the pore formation process has also been highlighted in ref 154. When side-chain charges of melittin peptides were removed, the peptides lost their ability to induce poration.

Nevertheless, it has to be emphasized that the electric charge alone is insufficient for pore formation. Marrink et al.¹⁵⁴ simulated interactions of KALP, a nonantimicrobial peptide (a net charge of +4) with lipid membranes and found no signs of pore formation. This shows that other properties of AMPs, such as the amphipathicity and peptide-peptide interactions that underpin cooperativity, are also essential. As for the nonantimicrobial *cationic* peptides, it is however still unclear whether a further increase in concentration of such peptides in solution (and a corresponding increase in a net charge accumulated nearby one of the membrane monolayers) could promote pore formation.

Another family of small cationic peptides which have been studied computationally are the so-called cell-penetrating peptides (CPP).¹⁵⁸ These relatively short peptides are able to penetrate cell membranes in an energy-independent manner; this makes them very attractive candidates as vectors for drug delivery.^{159,160} In contrast to the AMPs discussed above, the cell-penetrating peptides do not have well-defined hydrophilic or hydrophobic surfaces.

Atomic-scale molecular dynamics simulations have been employed to study interactions of model lipid membranes with three representatives of the CPP family: penetratin,¹⁶¹ the HIV-TAT peptide,^{161,162} and poly arginine peptide Arg-9.¹⁶³ All these peptides carry a considerable net charge under physiological conditions. Herce and Garcia¹⁶² studied the effect of the TAT peptide on phospholipid bilayers over a wide range of temperatures and peptide concentrations. They found that, at high concentrations of TAT peptides in solution

(protein/lipid ratio amounted to 1/18), one witnesses formation of nanometer-sized transmembrane pores through which the peptides translocate across the membrane.

The mechanism of TAT peptide translocation revealed in ref 162 involves strong interactions of the TAT peptides adsorbed on one membrane leaflet with lipid phosphate groups on both (proximal and distal) sides of the bilayer. As a result, the bilayer becomes thinner and the charged side chains of peptides start penetrating deep into the lipid bilayer, eventually nucleating formation of a hydrophilic pore. Once the pore is formed, the TAT peptides translocate across the bilayer by diffusing via the pore walls. A very similar picture was revealed in the simulations of a phospholipid bilayer interacting with four copies of Arg-9 peptide.¹⁶³ Interestingly, in contrast to rather stable pores formed by AMPs¹⁵¹ and to Arg-9 peptide-induced pores which stayed open for half a microsecond,¹⁶³ the pores induced by the TAT peptides were found to get closed after a few peptide molecules diffuse through the bilayer.¹⁶²

Recently, Yesylevskyy et al.¹⁶¹ reported extensive MD simulations in which no signs of CPP-induced pore formation were observed for either the TAT peptide or penetratin. Instead of pore formation, an alternative mechanism for penetration of such peptides across the membrane was proposed: Large deformations induced by the peptides in the lipid bilayer can eventually lead to the formation of a small vesicle within the cell that encapsulated the peptides (micropinocytosis).¹⁶¹ It was argued that the pore formation reported in ref 162 was observed because the simulation conditions deviated significantly from those normally employed in experiments (very high protein/lipid ratios and/or elevated temperature) and the electrostatic interactions were not handled properly. The latter issue might have tremendous impact in this particular situation and raises an important question regarding possible electrostatics-related artifacts in the simulations of highly charged objects nearby the lipid/water interface in general. Indeed, refs 151, 154, 162, and 163 considered cationic peptides without the inclusion of counterions. Such an approach potentially leads to artifacts because a simulation box now has a nonzero electric charge. Possible artifacts were minimized in refs 151 and 154 by the use of the reaction field approach. In this case the absence of counterions had only a minor effect, making interactions between cationic peptides and the lipid membrane somewhat stronger: Marrink¹⁵⁴ et al. demonstrated that the explicit inclusion of counterions slows down the overall process of pore formation, while the sequence of events is similar to that observed for a system with no counterions. The origin of this slowing down is in the effective screening of the peptide charges by counterions.

The artifacts become more pronounced when the particle-mesh-Ewald (PME) method is employed for the membrane/peptide systems without counterions.^{162,163} In particular, a nonzero net charge of a simulation cell could lead to the appearance of an extra electric field across the original cell. Indeed, such an additional substantial field was most likely observed in ref 162, as evidenced by a significant increase in the area of a bilayer. Similarly, an extensive bilayer expansion was found in membranes under a strong transmembrane electrostatic field caused by an ionic charge imbalance across the bilayer.^{76,77} Remarkably, this bilayer expansion vanishes when counterions are added to the membrane/peptide system.¹⁶¹ This finding highlights the

importance of neutralizing the system under study to avoid possible artifacts when the PME method is employed.

Apart from the atomistic models, molecular models of lower resolution (coarse-grained representations) have also been employed to study interactions of pore-forming peptides with lipid membranes. Marrink et al.¹⁶⁴ recently reported a multiscale approach that combined both atomistic and coarse-grained descriptions. Starting with the atomistic representation of a DPPC bilayer and magainin-H2 peptides in the water phase, they followed binding of the peptides to the membrane surface and subsequent pore formation.¹⁵¹ After the pore was formed, the atomistic representation was transformed to the coarse-grained one and the simulations were extended for 24 μ s. It was shown that the coarse-grained simulations (based on the MARTINI model) predict a fully hydrated, disordered, toroidally shaped pore which is similar to what was observed in atomistic simulations (although the size of the pore was somewhat smaller in the coarse-grained representation). It was also demonstrated that coarse-grained magainin-H2 peptides preinserted into a DPPC bilayer became aggregated and formed a pore in the bilayer. However, no pore formation was observed when CG magainin-H2 peptides were initially placed in aqueous solution nearby a DPPC bilayer, even at elevated peptide/lipid ratio.¹⁶⁴

Overall, the current state of the coarse-grained models is such that their applicability is limited as far as insertion of charged peptides (e.g., AMPs) into a membrane from aqueous solution is concerned. The main reason for that is the coarse-graining of water that is a key player in cationic peptide-induced pore formation. This definitely affects the partitioning of polar compounds into a low dielectric medium (the hydrophobic core of the membrane). As one of the important consequences, in coarse-grained simulations, the charged residues lose their hydration shell when they get embedded deep into the bilayer.⁴⁵ What is more, the free energy barriers for movement of charged and neutral Arg side chains across the lipid bilayer were found to be almost the same¹⁶⁵ when the coarse-grained model by Marrink et al.⁴³ was employed. To the best of our knowledge, there have been no coarse-grained simulations that report on pore formation due to adsorption of cationic peptides from solution to a lipid bilayer of standard thickness (such as a DPPC bilayer). Recently, self-assembly of magainin-H2 peptides and phospholipids randomly distributed in water was studied by coarse-grained simulations;⁴⁵ the authors observed a toroidal pore that was reminiscent of what was reported through atomic-scale simulations.¹⁵¹ However, direct observation of the pore formation due to adsorption of magainin-H2 from a coarse-grained water phase onto the membrane was lacking. Sansom et al.¹⁶⁶ used a coarse-grained approach to study the interaction of lipid membranes with another representative of cationic AMPs, maculatin 1.1 (a net charge of +3). Pore formation was not observed in this study either, most likely indicating limitations of the coarse-grained approach in general. The only way to promote pore formation due to charged CG AMPs in solution was to considerably reduce the thickness of the bilayer, thereby lowering the energy barrier associated with opening of a water pore.¹⁶⁴

For neutral pore-forming peptides, a coarse-grained level of description is proving to be more suitable. Three recent examples include coarse-grained MD simulations of lipid membrane systems with antimicrobial peptide alamethicin¹⁶⁷ and synthetic leucine-serine peptides^{168,169} LS3 and

(LSSL₂SL)₂. In the case of alamethicin, the peptide helices were preinserted into a bilayer perpendicular to the bilayer surface and their subsequent assembly into a bilayer spanning pore followed.¹⁶⁷ Interestingly enough, the pore was found to be too narrow for permeation of coarse-grained water particles and the model had to be reverted to an atomic-scale representation in order to be able to detect pore-mediated water leakage. As for the LS3 peptides, the peptides were placed randomly in solution and the subsequent CG simulations witnessed adsorption of peptides onto the membrane and spontaneous formation of a structure that can be classified as a barrel-stave pore.^{168,169} The resulting pore turned out to be large enough to get filled with a few coarse-grained water particles. In turn, (LSSL₂SL)₂, being a shorter version of LS3, shows a much lower propensity for poration compared to LS3. In this case, pore formation is observed when (LSSL₂SL)₂ peptides are initially placed in the bilayer rather than in the water phase.¹⁶⁹ The pore itself was found to be less stable, disordered, and close in shape to toroidal pores, which were previously observed for magainin-H2.^{45,151,164}

3.7. Pore Formation Induced by Cationic Polymers

The above-mentioned computational studies of the modes of action of antimicrobial peptides suggest that one can expect distortion of the bilayer membrane structure each time a sufficiently large net charge gets accumulated nearby the membrane surface. Therefore, any highly charged molecular species could be considered as a potential candidate for modulating the membrane structure. As an example, water-soluble synthetic polycationic polymers are indeed known to induce structural defects in cell membranes and to enhance the permeability of the membrane.^{170,171} Important representatives of such polymers are dendrimer macromolecules,¹⁷² which have been extensively employed for biomedical applications both as nanocontainers and as surface-active colloidal particles. They have a unique symmetric branching structure which allows one to directly control the size, shape, interior density, and surface functionality of the dendrimer. In particular, the terminal amine groups of polyamidoamine (PAMAM) dendrimers get protonated in aqueous solution under physiological conditions,¹⁷³ so that the dendrimers are characterized by a high positive surface charge. Combined with relatively low toxicity of the dendrimers, this makes them suitable for the effective compaction and protection of linear polyelectrolytes of the opposite charge (e.g., a nucleic acid strand) and for the permeabilization of cell membranes. As a result, PAMAM dendrimers are being considered as synthetic delivery vectors for DNA^{174–176} and for a variety of small drug molecules such as the anticancer drug cisplatin.^{177,178}

Given the dendrimers' exceptional potential for numerous biomedical applications, it is not surprising that cationic dendrimers and their interactions with biomembranes have attracted considerable attention. On the computational side, while the properties of individual dendrimers have been extensively studied over the past two decades, the first simulation studies of charged dendrimers interacting with cell membranes have emerged only very recently.

The simplest approach to model the "dendrimer–membrane" system is to model the membrane as a charged impermeable plane. This allows one to study the conformation changes of a dendrimer¹⁷⁹ or its complex with a linear polyelectrolyte¹⁸⁰ upon adsorption onto the membrane.

However, to understand dendrimer-induced changes in membranes, more involved models need to be invoked.

Recently, Kelly et al. published a series of papers^{181–183} where both a PAMAM dendrimer of third generation and a phosphatidylcholine membrane were treated on an atomic level. The computational cost was greatly reduced by considering implicit solvent with a spatially dependent dielectric constant. Since a lipid bilayer structure cannot be preserved in the absence of explicit water molecules, the authors had to impose hard-wall boundary conditions. Such an approach confines the mobility of lipid molecules and therefore limits the relevance of the model to studies of the dendrimer-induced structural changes in membranes. The authors were able to study the initial binding of G3 PAMAM dendrimers to a phospholipid bilayer and demonstrated that the binding is greatly enhanced for the charged dendrimers as compared to their neutral counterparts due to the strong interactions between charged dendrimer moieties and polar lipid headgroups.^{181,182} The dendrimers pronouncedly flatten upon binding, showing a large increase in asphericity and radius of gyration. Furthermore, the dendrimer binding was shown to induce a depression in the fluid phase bilayer, which is partially lined by lipid headgroups. Lipid molecules were rearranged in such a way that the hydrophobic dendrimer moieties were accessible to the hydrocarbon lipid chains without giving up the interactions between the protonated amine groups of the dendrimer and the lipid headgroups.¹⁸²

While providing valuable atomic-scale insight into the initial binding of charged dendrimers to phospholipid membranes, the aforementioned studies do not account for an explicit solvent and focus mostly on the dendrimer macromolecules of small size (low generation),^{181–183} clearly indicating the limitations for applying atomistic models to the problem at hand. Normally this is the situation when more coarse-grained models come into play.

Lee and Larson extended the original MARTINI model^{43–45} to dendrimer macromolecules in aqueous solution and performed an extensive series of coarse-grained MD simulations of lipid bilayers in the presence of charged dendrimers.^{184–187} The use of a coarse-grained approach allowed them to follow the system evolution over much longer times compared to what was accessible with the models of higher resolution. The authors showed that, upon initial binding, protonated dendrimers are able to either insert to the membrane, inducing dendrimer-filled pores, or deform the membrane. The outcome depends on the dendrimer size, on the dendrimer concentration, and on whether membrane undulations are suppressed.

In the latter case, when the membrane undulations are suppressed due to a relatively small membrane patch being considered, the dendrimer's ability to insert into the bilayer and to form pores turns out to depend on the size of a cationic dendrimer or, in other words, on its overall electric charge. In particular, it was shown that protonated, fifth generation (G5) PAMAM dendrimers are able to induce pores in the membrane while third generation dendrimers are not.¹⁸⁴ In accordance with the observations provided by atomic-scale models,^{181,182} the initial binding of dendrimer macromolecules is driven by the interaction between charged terminal beads of a dendrimer and polar lipid headgroups. The larger a dendrimer is, the deeper its charged moieties penetrate into the lipid/water interface after a dendrimer's insertion into the bilayer, so that they can eventually make contact with

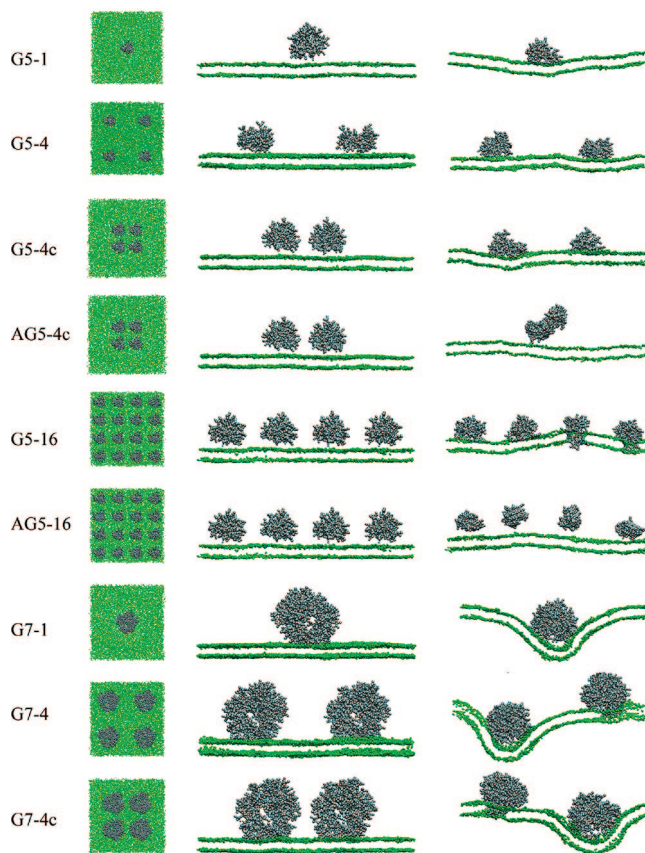


Figure 7. Fifth (G5) and seventh (G7) generation PAMAM dendrimers of different concentrations interacting with a lipid bilayer. All dendrimers are protonated except those marked as AG (fully acetylated dendrimers). Shown are snapshots of the top view (left images) and the side views at the beginning (middle images) and at the end ($t = 160$ ns, right images) of simulations. Dendrimers are shown in gray and the lipid headgroups in green; water molecules, lipid tails, and ions are not shown. Reproduced with permission from ref 185. Copyright 2008 American Chemical Society.

the lipid headgroups of the opposite leaflet. This is indeed seen for a G5 dendrimer (but not for a G3 one).¹⁸⁴ Once the first charged dendrimer groups reach the opposite side of the membrane, a transmembrane pore filled with the dendrimer forms and the system relaxes to the equilibrium state at which the dendrimer gets inserted symmetrically into the bilayer. Since the location of charged dendrimer groups in the hydrophobic core of the membrane is very unfavorable, they get localized within the lipid/water interface, while uncharged groups are inside the membrane. Pore formation is not observed when the dendrimers are uncharged (acetylated) and the dendrimer charge is either insufficient (dendrimers of low generation) or screened due to addition of salt.¹⁸⁴

When undulation modes are not suppressed, i.e. the bilayer patch is large enough, the dendrimer concentration becomes crucial. At low concentrations (a single cationic dendrimer in the vicinity of the membrane), the dendrimers induce a deformation of the membrane rather than pore formation, with the deformation being more pronounced for larger dendrimers; see Figure 7. This holds for dendrimers of up to generation seven.¹⁸⁵ In contrast, increased dendrimer concentration is able to promote pore formation: Adsorption of multiple copies of charged dendrimers reduces the flexibility of the membrane, rendering the situation similar to what was observed for small bilayer patches. This effect

is more pronounced for dendrimers of large size. In particular, for G7 PAMAM dendrimers, some of the dendrimer molecules induce significant bilayer bending with negative curvature, while others reside next to these dendrimers on regions with positive curvature and tend to induce pore formation;¹⁸⁵ see Figure 7. Furthermore, no sign of aggregation between the different protonated dendrimers prior to their adsorption onto the membrane was observed, most likely due to the strong electrostatic repulsion between highly charged dendrimer molecules.¹⁸⁵

Interestingly, the effect of charged dendrimers on lipid membranes turns out to differ considerably from the corresponding effect of linear polyelectrolyte chains. As demonstrated by Lee and Larson,¹⁸⁶ poly-L-lysine (PLL), a linear cationic polymer, was not able to induce pores within the time scales accessible in simulations despite the fact that the total charge of a PLL polymer was the same as that of a PAMAM dendrimer, which did porate the membrane. The explanation should be directly related to the differences in the shapes of linear PLL and spheroidal PAMAM polymers: A flexible PLL chain can easily spread on the membrane surface, interacting with lipid polar headgroups of one leaflet only. In contrast, considerably more rigid PAMAM dendrimers (especially dendrimers of high generations) cannot spread on one leaflet and have to get inserted in the membrane interior and interact with the lipid headgroups on both sides of the membrane.¹⁸⁶ In other words, it is the branched topology of a dendrimer which accumulates charges within a compact object and induces local membrane rupture.

Yan and Yu have employed dissipative particle dynamics and studied interactions of lipid membranes with charged dendrimers;^{188,189} the resolution of their coarse-grained model was similar to that provided by the MARTINI force-field. The authors systematically varied the strength of interactions between hydrophilic dendrimer groups and polar lipid headgroups as well as between hydrophobic dendrimer beads and lipid tails. They found that increasing the attraction between the outer-dendrimer hydrophilic component and the lipid headgroups leads to wider spread of the dendrimer on the membrane surface but has a minor effect on the insertion of the dendrimer into the membrane. The latter is controlled to a great extent by the attractive interactions between the inner-dendrimer uncharged groups and hydrocarbon lipid chains.¹⁸⁸

The above studies were also extended to the lipid bilayers under tension.^{188,189} It turns out that adsorption of charged PAMAM dendrimers of generation 5 and higher onto the lipid bilayer noticeably reduces the critical surface tension required for membrane rupture. In other words, charged dendrimers can induce pore nucleation at a surface tension which is lower than that required for rupture of a dendrimer-free membrane.¹⁸⁹ This effect could most likely be due to the strong attraction between the uncharged interior of an adsorbed dendrimer and lipid tails, which creates lipid-poor regions on the membrane surface nearby the dendrimer, partly disrupts the ordered lipid arrangement in the bilayer, and weakens the energy barrier for pore formation.^{188,189}

3.8. Pore Formation due to Lipid Peroxidation

The destabilization of the bilayer structure with subsequent promotion of defect formation can also be triggered by modification of lipid hydrocarbon tails. This can happen, for example, due to lipid peroxidation. As such, lipid peroxidation, i.e. the oxidative degradation of lipids, plays an

important role in damage of cell membranes, as it alters their physiological functions and is therefore relevant to cellular aging and to a variety of diseases.¹⁹⁰ One of the most dramatic effects of lipid peroxidation on the structural properties of membranes is in the increased membrane permeability, which may enhance leakage of various solutes through the membrane, disrupt the ion gradient, and alter metabolic processes.¹⁹¹ However, the exact molecular mechanism of the membrane damage due to lipid peroxidation is still not clear.

On the computational side, this problem has been addressed with the use of atomic-scale MD simulations.⁹⁴ The authors⁹⁴ focused on the effect of lipid peroxidation on the properties of palmitoyl-linoleyl-phosphatidylcholine (PLPC) lipid bilayers. In particular, the *sn*-2 linoleate chain in a PLPC lipid was replaced with one of four oxidation products of linoleic acid, containing either a hydroperoxide or an aldehyde group in two different positions in the lipid tails. The concentration of the oxidized lipids in a PLPC bilayer was systematically varied from 2.8 to 50%.

It turns out that the oxidized functional groups change the conformational properties of the lipid tails: As the tails become more polar due to the presence of aldehyde or hydroperoxide groups, they bend toward the water phase and hydrogen-bond with water and the lipid headgroups. This results in an increase in the area per lipid and, correspondingly, in a reduction of the bilayer thickness, with the effect being more pronounced at high concentrations of oxidized lipids.⁹⁴ Overall, the bilayer becomes considerably more permeable, as demonstrated through the calculation of the potential of mean force for water. Remarkably, at concentrations of oxidized lipids higher than 5%, formation of water pores is observed.⁹⁴ The size of the water defects is found to correlate with the average area per lipid: The higher the area per lipid, the larger the defect radii. In turn, higher area per lipid is observed for oxidized lipids which have polar oxygens closer to the terminal methyl group of the lipid tail.⁹⁴

All in all, an increase in polarity of lipid tails due to oxidation makes the lipid bilayer prone to water defect formation, especially at high concentrations of oxidized lipids. Vernier et al.⁹³ have demonstrated that this increase in membrane permeability leads to the fact that lipid bilayers containing oxidized lipids can be electroporated more easily compared to their nonoxidized counterparts. The simulations of PLPC bilayers have shown that poration time drops significantly when the fraction of oxidized lipids in a bilayer increases and that the site of electropore formation was always associated with one or more oxidized lipids.⁹³

3.9. Energetics of Pore Formation in Lipid Membranes

The above sections clearly demonstrate that in most cases one needs to expose a lipid membrane to rather strong external destabilizing factors (electric field, mechanical stress, shock waves, surface-active molecules, highly charged solutes) to cause pore formation. The high energetic costs of pore formation are consistent with a fundamental biological role of the cell membrane to serve as a barrier around the cytoplasm. In particular, this also implies that the formation of a pore in an unperturbed lipid bilayer due to thermal fluctuations is an unlikely event.^{192,193} Insight into the energetics of pore formation could give important information regarding the basal permeability of cell mem-

branes to ions, lipids, and other species which are known to passively cross membranes through hydrophilic transient pores.

Theoretical ideas of pore formation in membranes are dominated by classical nucleation theory. The model assumes the membrane to be a two-dimensional elastic medium with a hole.¹⁹² The medium is characterized by a free energy per unit area (surface tension) γ , while the hole edge is characterized by a free energy per unit length or line tension Γ . The stability of a hole of radius r is given by the interplay between the positive, edge free-energy (which is proportional to the pore perimeter) and the loss in the surface-area free energy (which is proportional to the area of the hole) due to the formation of the hole; that is, $\Delta G = 2\pi r\Gamma - \pi r^2\gamma$. The model yields an activation barrier of $G^* = \pi\Gamma^2/\gamma$ and predicts that pores with a radius below a certain critical value are unstable while those above this radius will grow indefinitely until the membrane ruptures.¹⁹² Further refinements of the model incorporate curvature energy in addition to surface tension¹⁰⁸ and the effect of fluctuating undulations and the entropy associated with pore shape.¹⁹⁴ The refinement of Tolpekina et al.¹⁰⁸ suggests that there is a local minimum just past the critical radius above which the free energy increases with an increase in pore size, hence explaining the formation of metastable pores (note that the simulations with constant bilayer area were considered in ref 108).

Since the probability of spontaneous pore formation in unperturbed lipid membranes is extremely low, the conventional molecular dynamics technique is not a suitable tool for studying such processes; the so-called constrained MD simulations have to be used instead, which allow one to measure the free energy cost of pore formation. In practical terms, two different methods for calculating the free energy of pore formation have appeared in the literature.

One of the methods utilizes the local lipid density in the center of a bilayer as a reaction coordinate to be constrained. The corresponding repellent cylindrical potential is applied only to the hydrocarbon tails of lipid molecules (but not to the headgroups). The method was first used for calculating the free energy of pore formation in lipid bilayers built from coarse-grained amphiphilic molecules.^{195,196} Wohlert et al.¹⁹⁷ applied it to a DPPC lipid bilayer modeled at an atomic-scale resolution. The authors calculated the free energy of pore formation as a function of pore radius and showed that one could identify two regions in the free energy dependence on pore radius: quadratic for radii less than 0.3 nm and approximately linear for larger pores (although some curvature is observed for large pores with $r > 1$ nm). The threshold radius value of 0.3 nm corresponds to the first appearance of pores filled with water.¹⁹⁷ The corresponding free energy, being in fact the free energy of the formation of water-filled pores, was found to be around 90 kJ/mol. It is pertinent to note that the pores observed in a DPPC lipid bilayer were hydrophilic, i.e. were lined with polar lipid headgroups which redistributed toward the bilayer interior.¹⁹⁷

Notman et al.¹⁹⁸ applied the method to study the transmembrane pore formation in bilayers built from ceramide 2 lipids, as such bilayers are considered as a model for the upper layer of skin (stratum corneum). In contrast to PC lipids, ceramide molecules are densely packed due to hydrogen bonding, so that the corresponding bilayer is in the gel phase under physiological conditions. This dramatically affects the overall process of pore formation: one can observe pores as small as 0.03 nm in radius.¹⁹⁸ The pores,

however, turned out to be hydrophobic: redistribution of the polar lipid headgroups toward the bilayer interior is prevented by strong H-bonds between lipids. The energy cost of the formation of such pores is found to be more than an order of magnitude higher than that for a fluid DPPC bilayer.¹⁹⁸ This is a clear indication that pore-mediated transport across the stratum corneum under standard conditions is very unlikely. Remarkably, at all considered radii, the authors observed vapor (not filled with liquid water) pores only. It is likely that a further increase in the pore size would eventually lead to water filling of the pores similar to what was observed in the studies of water permeation through hydrophobic nanopores.^{199–202} Indeed, preliminary tests showed that when the largest studied pore (1.3 nm in radius) was forced to be filled with water, the water molecules remained in the pore.¹⁹⁸

The idea that condensed phases of lipids can promote hydrophobic pores is not only relevant to skin lipids dominated by ceramides but might also be applicable to lipid raft structures that have a more condensed character relative to lipid membranes in the fluid phase. This finding that small porelike hydrophobic defects do not compromise the membrane's barrier function to small polar molecules and ions is highly significant. The implication is that, for a membrane in a condensed state, it need not be perfectly contiguous to maintain its barrier function. This view explains the apparent paradox that the human body should have evolved to employ rigid (gel) phase ceramide-based lipids to serve as the barrier between the body and the outside, while such a rigid phase is expected to be highly prone to defects whenever the skin undergoes flexing. The hydrophobic defects that result do not compromise the barrier with respect to water loss. Meanwhile, in condensed phases such as lipid rafts, any defects at the condensed fluid phase or protein-condensed phase boundaries (introduced due to regular turnover of the lipids or protein incorporation) are expected to be hydrophobic and, hence, are not expected to compromise the membrane barrier to small polar molecules and ions.

The extremely high energy required to induce a pore in ceramide bilayers might be a generic feature of any lipid bilayer in the gel phase characterized by dense packing and limited mobility of lipid molecules. Turning the bilayer to the fluid phase should facilitate pore formation considerably. This was nicely illustrated in ref 198 when ceramide bilayers were solvated in water/dimethylsulfoxide (DMSO) solvent. The authors employed a rather high DMSO concentration, 60 mol % (lipid-free basis), which was shown to induce a transition in the ceramide bilayers from the gel phase to the fluid phase.²⁰³ They found that the free energy barrier of pore formation in the DMSO-fluidized ceramide bilayers was around 10 kJ/mol; that is, it dropped by almost 2 orders of magnitude as compared to the case of the bilayers without DMSO (the gel phase). Interestingly, the resulting pores were hydrophilic and filled with water and DMSO.¹⁹⁸

Marrink et al.^{204,205} utilized a similar constrained dynamics approach to speed up the equilibration of lipid vesicles. After initial aggregation of lipids, such an equilibration requires adjusting the numbers of lipid molecules in the inner and outer leaflets, so that some lipids should translocate across the bilayer. This can be facilitated by the insertion of temporary hydrophilic pores in a lipid vesicle by means of, for example, application of the repellent cylindrical potential mentioned above.^{204,205}

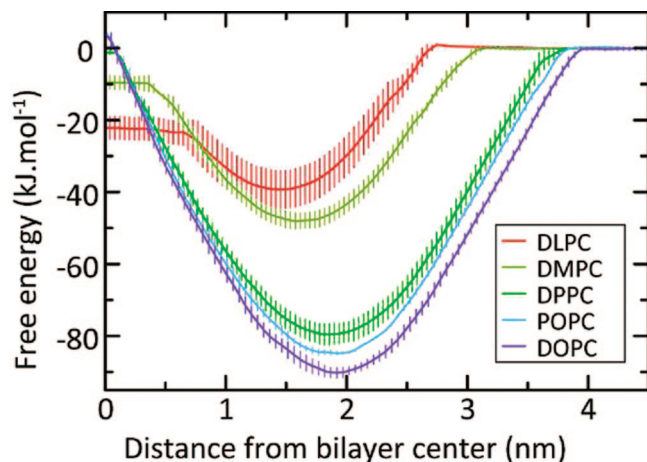


Figure 8. Potential of mean force for a lipid for DLPC (red), DMPC (yellow), DPPC (green), POPC (blue), and DOPC (violet) bilayers. The distance refers to the position at which the phosphate group of a lipid is restrained with respect to the bilayer center. For ease of comparison, the PMFs were arbitrarily set to zero in bulk water. Reproduced by permission of The Royal Society of Chemistry from ref 207 (<http://dx.doi.org/10.1039/b902376c>).

An alternative indirect approach for characterizing the free energy of pore formation was proposed by Tieleman and Marrink.²⁰⁶ The authors calculated the potential of mean force (PMF) of phospholipids in a lipid bilayer by umbrella sampling using molecular dynamics simulations. The umbrella potential was applied to the center of mass of the phosphate group of a DPPC lipid, so that the lipid was constrained at different positions within the lipid bilayer. The resulting PMF was found to rise steeply as the lipid moves toward the bilayer center due to the interaction between the polar PC headgroup and the hydrophobic core of the bilayer. A similar steep rise in the PMF is observed when the lipid moves into the bulk water due to low solubility of the lipid's hydrocarbon tails; see Figure 8. The difference in the free energy of a DPPC lipid in its equilibrium position and in the middle of the bilayer was found to be around 80 kJ/mol.²⁰⁶ Remarkably, when the headgroup of DPPC was constrained in the middle of the bilayer, the authors witnessed the formation of a small water pore. Since the PC headgroup is polar with a positive charge on the choline group and a negative charge on the phosphate group, placing it in the hydrophobic membrane core causes deformations of the bilayer, so that water molecules and lipid headgroups could enter the interior of the bilayer and prevent desolvation of a hydrophilic polar moiety. The resulting pore is hydrophilic and included a water file spanning the entire DPPC bilayer and headgroups of adjacent lipids lining the water file.²⁰⁶ Therefore, it was concluded that the free energy of moving a lipid across the bilayer is also an energy cost of forming a water pore. The evaluated value for the free energy of pore formation (80 kJ/mol) is close to the results of Wohlert et al.,¹⁹⁷ who reported values in the range from 75 to 100 kJ/mol for a DPPC bilayer.

Later Tieleman et al.²⁰⁷ extended the PMF calculations to single-component bilayers comprised of dilauroyl-phosphatidylcholine (DLPC) and dimyristoyl-phosphatidylcholine (DMPC), lipids which have shorter acyl chains compared to DPPC (the length of lipid chains decreases as follows: DPPC > DMPC > DLPC). It was found that the free energy barrier of pore formation depends strongly on the length of the lipid acyl chains. In particular, the values of 16 and 40 kJ/mol were reported for the free-energy of pore formation

in DLPC and DMPC lipid bilayers, respectively.²⁰⁷ These values are considerably smaller than the 80 kJ/mol found for DPPC bilayers.²⁰⁶ Interestingly, the size of a water pore turns out to be larger for thinner bilayers. When a lipid was constrained in the center of the bilayer, the average radius of the pore was reported to be 0.95 nm, 0.86 nm, and 0.55 nm for DLPC, DMPC, and DPPC lipid bilayers, respectively. These findings clearly demonstrate that the shorter the lipid tails are, the lower the free-energy barrier for pore formation is, and also the larger the resulting pore becomes.²⁰⁷ It is instructive to note that for bilayers built from lipids with longer chains as well as for DPPC bilayers with cholesterol, no pore formation has been observed when a lipid was pulled through the bilayer;^{207,208} see the discussion in section 5.1.

Similar PMF calculations have also been performed with the use of the coarse-grained MARTINI model.⁴⁴ While the general feature of the PMF profile turned out to be very similar to that extracted from atomic-scaled MD simulations, the coarse-grained model gives larger values for the free-energy barrier: 90 vs 80 kJ/mol for a DPPC bilayer and 75 vs 16 kJ/mol for a DLPC bilayer. However, the most dramatic difference was the absence of pore formation when a DPPC lipid and a DLPC lipid were dragged through the corresponding bilayers. This was attributed to the major simplifications made in the coarse-grained model related to a uniform dielectric constant of the entire system.⁴⁴ Most recently, Xing and Faller²⁰⁹ employed the PMF calculations to evaluate the density imbalance between two leaflets of a supported lipid bilayer.

4. Trafficking of Salt Ions across Protein-Free Lipid Membranes

Transport of salt ions across cell membranes is essential for many cellular functions and represents one of the long-standing problems in membrane biophysics. In living cells, the ion transport is mainly governed by specialized proteins such as ion channels and pumps. However, biological membranes themselves are not perfect barriers, as ions can permeate the cell membrane unassisted.^{5,6} Such an unassisted ion transport is of prominent interest because any ion leakage across the membrane is coupled to energy transduction and cellular function.

In general, two different mechanisms have been proposed for the unassisted ion transport across a protein-free lipid membrane: the solubility-diffusion mechanism, and the pore-mediated mechanism. The first mechanism means that ions (along with their hydration shells) partition into the hydrophobic core of a membrane and diffuse across the membrane interior.²¹⁰ Alternatively, ion trafficking across membranes can greatly be facilitated by the formation of transient water pores.^{5,6} The specific mechanism seems to depend on both ion type and membrane thickness. It has been shown experimentally that for potassium ions (and most likely for other alkali ions) permeation across thin membranes (comprised of lipids with the acyl tail length from 14 to 18 carbon atoms) follows the pore-mediated mechanism, while the solubility-diffusion mechanism is identified for thicker lipid membranes.⁹ In contrast, permeation of halide ions was found to depend only slightly on the membrane thickness and to be consistent with the solubility-diffusion mechanism.²¹¹ On the computational side, ion trafficking across lipid membranes has been studied via the application of biased simulations wherein an ion is dragged through membranes

and by unbiased MD simulations of lipid membranes with preformed pores.

4.1. Defect-Mediated Ion Permeation without Actual Pore Formation

There have been a number of computational studies where biased MD simulations were employed to get insight into the molecular mechanism of the permeation of ions across protein-free lipid membranes. These studies focused on dragging an ion through the membrane: Constraining an ion at a series of different positions across the membrane gives access to the free-energy barrier for ion permeation.

In a pioneering work, Wilson and Pohorille²¹² studied permeation of sodium and chloride ions across a glycerol 1-monoleate (GMO) membrane, with the ions being restrained within the membrane with the use of adaptive biasing potential. The authors found that when ions enter a membrane, they keep water molecules from their first hydration shells. Upon approaching the membrane center, the hydration of an ion decreases. The ion gets solvated with GMO headgroups that replace water molecules from the first hydration shell of the ion, making the total solvation number of the ion almost unchanged.²¹² Remarkably, the movement of an ion toward the membrane interior induced the formation of a transient water defect on the side from which the ion entered the membrane. Once the ion had crossed the midplane of the membrane, the defect switched sides and developed on the opposite side of the membrane.²¹² We note that the formation of a defect spanning the entire membrane has never been observed in the study. Therefore, it was concluded that ion permeation through the GMO membrane occurs according to the solubility-diffusion mechanism but not through water pores. The calculated free-energy barriers were found to be quite high: 226 and 211 kJ/mol for Na⁺ and Cl⁻ ions, respectively.²¹² It should be noted that the simulation time per umbrella window was rather short and, therefore, convergence of the free-energies can be debated.

A decade later, Tepper and Voth reported a series of computational studies of permeation of protons and sodium ions across lipid membranes.^{213,214} In particular, umbrella sampling has been employed to evaluate the free-energy barrier of Na⁺ ion permeation across a dimyristoyl-phosphatidylcholine (DMPC) lipid bilayer. The sequence of events was very reminiscent of that found by Wilson and Pohorille:²¹² Dragging a sodium ion across a membrane led to the development of a water defect on the corresponding side of the membrane, and polar PC headgroups were also involved in the formation of the defect. When the ion had crossed the middle of the bilayer, the initial defect disappeared and became replaced with a similar defect developed on the opposite side of the bilayer. The height of the free-energy barrier of a Na⁺ ion permeating across a DMPC membrane was found to be around 100 kJ/mol.²¹⁴ Although a water defect spanning the entire membrane was not observed in ref 214, the authors claimed that it could be observed for thinner bilayers which would be characterized by lower free-energy barriers.

Recently, the potential of mean force (PMF) for permeation of Na⁺ and Cl⁻ ions across a DMPC membrane was evaluated in ref 215 with the use of biased molecular dynamics simulations. The study confirmed the overall picture observed in earlier simulations: restraining an ion within a lipid bilayer leads to formation of a water finger that originates from the closest membrane side. When the

ion reached the center of the membrane, the water finger switched from one leaflet to the other. The PMF calculations gave the following barriers for ion permeation: 91.6 kJ/mol for Na⁺ and 98.7 kJ/mol for Cl⁻ ions.²¹⁵ Note that the energy barrier for Na⁺ ion permeation is rather close to that reported by Tepper and Voth.²¹⁴ The authors also addressed the problem of whether ion pairing facilitates the permeation across phospholipid bilayers. As the PMF for the permeation of a Na-Cl pair was computed, the corresponding energy barrier was found to be 115.5 kJ/mol, which is higher than the barriers for the individual Na⁺ and Cl⁻ ions.²¹⁵ Therefore, pairing of ions does not lower the energy required for ion permeation through a lipid membrane, in line with theoretical predictions by Parsegian.²¹⁶

It should be emphasized at this point that the formation of water defects due to an ion crossing the membrane has a generic nature; similar effects can also be observed upon insertion of other charge (polar) residues in the center of a lipid membrane. One of the examples—a polar lipid headgroup—was mentioned in section 3.9 when the calculation of the lipid PMF was discussed.^{206,207} Another important example is related to charged amino acids. Among others, arginine side chains have attracted particular attention because of their role in voltage-sensitive ion channels.²¹⁷ Molecular dynamic simulations of such ion channels showed that direct exposure of arginine-containing voltage sensors to the membrane interior caused considerable water defects.^{218–220} Simulation studies of model transmembrane helices containing arginine residues also demonstrated that arginine did not desolvate completely and retained its hydration shell by pulling water molecules and lipid headgroups into the hydrophobic core of the membrane.²²¹ Similar water defects and membrane perturbations were also reported in the study by Dorairaj and Allen,²²² who calculated the free-energy profile for moving of a poly-leucine transmembrane helix that contained a protonated Arg side chain across a DPPC lipid membrane. To study the effect of arginine in more detail, several groups carried out calculations of the potential of mean force of arginine in the membrane environment.^{223–228} It turned out that dragging an ionized Arg side chain across a membrane causes formation of a water defect accompanied by the corresponding partial redistribution of lipid headgroups. Such defects (also observed for other charged amino acid side chains such as ionized forms of Asp, Glu, and Lys) were shown to be stable even when the side chain was placed in the center of the membrane.^{223,224} As for other examples of charged residues, one can mention a very recent MD study of partitioning of aspirin and ibuprofen, two nonsteroidal antiinflammatory drugs, in a DPPC lipid bilayer.²²⁹ The authors demonstrated that the anionic forms of the drugs permeate the bilayer with their polar groups completely hydrated. Their permeation is accompanied by the formation of water fingers that extend halfway up to the bilayer center and by the corresponding asymmetric thinning of the bilayer.²²⁹

Ion permeation is characterized by a very high energy barrier and therefore represents an extremely rare event. Such events cannot be studied by conventional unbiased simulations unless certain measures are undertaken to reduce the barrier. One way to do that is to apply a strong electric field to the bilayer system. This has been done in ref 77, where the electric field across DMPC bilayers was induced by a transmembrane ionic charge imbalance. When the imbalance was high enough, pore formation and subsequent ion transport across the bilayer were observed on a nanosecond

scale.^{76,77} However, it turned out that a potassium ion could permeate the bilayer without actual pore formation. Similar to the pore-mediated permeation, two water fingers first penetrated the membrane from both sides and met each other, forming a chain of water molecules which spanned the entire membrane. One of the water fingers came with a potassium ion, so that upon the formation of the water chain the K^+ ion shared both fingers. Very quickly the metastable water chain broke and the K^+ ion, being now a part of the opposite water finger, permeated through the membrane.⁷⁷ The process of K^+ permeation took around 50 ps and was an order of magnitude faster than the formation of a hydrophilic pore, which involves redistribution of massive lipid headgroups. Such permeation of a potassium ion without actual pore formation was observed in 2 (out of 20) simulations and was found to be insensitive to the details of the force-field employed for K ions (the Gromacs and Charmm force-fields were considered).⁷⁷

Another example of ion permeation across a membrane without actual pore formation is given in ref 143, where ethanol molecules were used to reduce the barrier for the formation of transient water defects. As discussed in section 3.5, when the ethanol concentration exceeds 12 mol %, formation of nonbilayer globular structures within the membrane interior is observed.¹⁴³ Remarkably, these micellar-like structures (see Figure 5) can serve as traps for hydrated salt ions. It was shown that the micellar structures containing Na^+ , K^+ , and Cl^- ions remain in the membrane interior for around 100 ns. Although a complete translocation event of an ion across the membrane was not observed due to limited simulation time, one could hypothesize that such ethanol-induced nonbilayer structures could play the role of carriers for salt ions in transporting them between the two sides of a phospholipid membrane.¹⁴³

4.2. Ion Transport through Preformed Water Pores

An analysis of the free-energy barriers of ions dragged across a lipid membrane and of the formation of transient water pores (see section 3.9) shows that ion permeation through relatively thin membranes is most likely pore-mediated. Indeed, the free-energy of pore formation in a DMPC bilayer was found to be 40 kJ/mol,²⁰⁷ while the energy barriers for dragging salt ions across a DMPC membrane were estimated to be much higher: 91.6 and 98.7 kJ/mol for Na^+ and Cl^- ions, respectively.²¹⁵ Tepper and Voth reported 100 kJ/mol for Na^+ ion permeation.²¹⁴ For thicker DPPC bilayers, the corresponding energy barrier of pore formation is around 80 kJ/mol²⁰⁶ and should also be smaller than the barrier for dragging ions across a DPPC membrane (the latter quantity for DPPC bilayers has to exceed ~ 100 kJ/mol reported for thinner DMPC bilayers). Thus, as far as the DMPC and DPPC bilayers are concerned, one can conclude that the pore-mediated permeation of ions across a membrane is more favorable energetically than the defect mediated pathway without actual pore formation (see previous section). Therefore, a direct study of the transmembrane ion permeation in DMPC and DPPC lipid bilayers is possible through considering the bilayers with *preformed* pores. Such computational studies have indeed been reported, with the hydrophilic pores having been induced by transmembrane ionic charge imbalance,^{76,77,80} surface tension,¹⁰⁶ and surface-active molecules.²³⁰

In the situation where the water pores are induced by a transmembrane ionic charge imbalance, the bilayer system is far from equilibrium. As illustrated in Figure 3A–F for a DMPC bilayer with NaCl salt, a sufficiently large charge imbalance of Na^+ ions on both sides of the bilayer leads to the formation of a transient water pore on a nanosecond time scale.^{76,77,79} After the water pore has become large enough, one observes the transport of sodium and chloride ions through the resulting pore along the Na^+ ion density gradient; see Figure 3G–J. Remarkably, the pore-mediated ion permeation and the size of the pore itself are both controlled by the ion-induced transmembrane potential.^{76,77,80} Higher potential difference between the two sides of a bilayer implies faster transmembrane ion leakage and a larger pore. Permeation of an ion across the membrane discharges the transmembrane potential difference and, therefore, slows down the rate of transmembrane ionic transport and decreases the size of a pore. Eventually, the pore becomes too small and the ion leakage stops; see Figure 3K.

Despite the fact that the pore-mediated ion transport in this case is driven by a strong electric field, certain features of the transport turn out to be generic and hold also in the absence of such a field. For the bilayer system with NaCl salt, sodium ions require smaller pores for permeation than chloride ions. However, no selectivity of DMPC bilayers with respect to Na^+ and Cl^- ion permeation has been observed.⁷⁷ The latter finding contradicts the results by Hansen et al.,^{231,232} who studied the electric field-driven ion transport through a hydrophobic pore and found that the free-energy for Na^+ ion permeation is lower than that for Cl^- ions. Therefore, there is a clear indication that there exists an additional factor which slows down transport of Na^+ ions across a phospholipid membrane. This factor is most likely the well established strong interactions of sodium ions with the carbonyl regions of PC lipid headgroups^{82,113–115} and, therefore, with the “walls” of the hydrophilic pores, which are lined by the lipid headgroups. In contrast, chloride ions do not bind to the lipid headgroups and remain in bulk water.^{82,113–115}

For DMPC bilayers with KCl, the situation is somewhat different. Potassium ions, being larger than sodium ions, bind only very slightly to the pore walls.^{77,115} Therefore, one can expect that the ion permeation in this case is mostly governed by the corresponding free-energy barrier. According to Hansen et al.,²³² the free-energy barrier for K^+ ions permeation through a hydrophobic pore is much smaller than the barrier for Cl^- ions. This finding indeed holds also for membrane pores, leading to a pronounced selectivity of protein-free phospholipid membranes with preformed water pores to potassium ions as compared to chloride ions: It turns out that three-fourths of all leaked ions are K^+ .⁷⁷ Further, the findings related to the pore-mediated permeation are found to be robust to a choice of the force-field parameters employed for the ions.⁷⁷

An alternative approach to preforming water pores in lipid bilayers is illustrated in ref 106, where one studied the transport of Na^+ and Cl^- ions through the tension-induced pores. By varying the surface tension applied, the authors focused on 3 types of water pores: small, medium, and large pores with corresponding average radii of 0.8 nm, 1.2 nm, and 1.8 nm.¹⁰⁶ Note that in this case there are no extra forces exerted on ions (such as electric field), so that diffusion of ions through the pores is driven by thermal fluctuations only. Similar to the case in ref 77, it was shown that sodium and

chloride ions permeate a preformed hydrophilic pore via a different mechanism. Due to the above-mentioned strong interaction between Na^+ ions and lipid headgroups, sodium ions adsorb onto the membrane surface and diffuse across the interface. In contrast, the chloride ions only slightly interact with a lipid membrane and therefore enter the middle of the pore from bulk water.

This difference in the permeation mechanism is clearly seen in the observed selectivity of the pores to Na^+ and Cl^- ions.¹⁰⁶ The selectivity strongly depends on the size of the pore. For the smallest pores (with the radius of 0.8 nm), no permeation events of Cl^- were observed while Na^+ ions permeated with unidirectional flux $j_{\text{Na}} \sim 0.005 \text{ ns}^{-1} \text{ nm}^{-2}$, allowing one to conclude that small pores are selectively permeable to Na^+ .¹⁰⁶ Increasing the radius of a pore from 0.8 to 1.2 nm (medium pores) does not increase the permeability rate of Na^+ ions. However, the size of the pore is now large enough for permeation of Cl^- ions which leak across the membrane at a rate even larger than that for Na^+ ions ($j_{\text{Cl}} \sim 0.02 \text{ ns}^{-1} \text{ nm}^{-2}$). Further expansion of the pore (large pores) leads to a reversal from sodium to chloride selectivity:¹⁰⁶ the Cl^- ion flux is found to be an order of magnitude larger than the flux of Na^+ ions, $j_{\text{Cl}} \sim 0.1 \text{ ns}^{-1} \text{ nm}^{-2}$ versus $j_{\text{Na}} \sim 0.01 \text{ ns}^{-1} \text{ nm}^{-2}$. These findings regarding ion selectivity are in fair agreement with the results of ref 77, where the radius of the pore in the bilayer system with NaCl salt was varied from 0.7 to 1 nm, i.e. was somewhat larger than the size of small pores considered by Marrink et al.¹⁰⁶ We note that large pores (~ 1.8 nm in radius) never developed in the bilayers studied in ref 77 due to fast pore-mediated ion leakage, which discharged the transmembrane potential, thereby reducing the size of the pore.

Based on the estimated microscopic flux of Na^+ ions across a hydrophilic pore, one can get access to the macroscopic permeability of ions through the phospholipid membrane. With the free energy of pore formation in a DPPC membrane at hand (which was estimated to be ~ 80 kJ/mol),²⁰⁶ Marrink et al.¹⁰⁶ found $10^{-13} \text{ cm s}^{-1}$ for the permeability coefficient of Na^+ ions. Remarkably, this value is comparable with the corresponding experimental data on the permeability rate of sodium ions through pure lipid bilayers.⁶ This strongly suggests that sodium permeation across protein-free phospholipid membranes occurs primarily via hydrophilic water pores.

We conclude this section with a discussion of ionic transport through water pores induced in lipid membranes by the amphiphilic solvent dimethylsulfoxide (DMSO).²³⁰ As mentioned in section 3.5, DMSO within a certain concentration range is able to induce formation of transient hydrophilic pores. To prove that these pores could serve as a pathway for ion permeation, Gurtovenko and Anwar²³⁰ considered DPPC bilayer systems with 10 and 15 mol % of DMSO (lipid-free basis), to which either NaCl or KCl salt was added. Note that the chosen DMSO concentrations induce water pores in salt-free DPPC membranes.¹²⁸ It was found that sodium ions, adsorbing on the membrane surface and forming tight complexes with lipid headgroups,^{82,113,115} prevent poration of a DPPC bilayer with 10 mol % of DMSO. This finding is in line with the results of Marrink et al.,¹⁰⁶ who demonstrated that adding NaCl salt destabilized a pore because the binding of Na^+ cations at the lipid/water interface increased the pore line-tension. Increasing the DMSO concentration to 15 mol %, however, leads to pore formation in a DPPC lipid bilayer with NaCl, so that one

can observe the pore-mediated ionic leakage driven by thermal fluctuations.²³⁰ Interestingly, the number of leaked Cl^- ions was about 40% larger than that of leaked Na^+ ions due to the above-mentioned strong interactions of sodium ions with lipid headgroups. In turn, for the DPPC bilayer systems with KCl, the pore formation and subsequent ion transport were witnessed at both (10 and 15 mol %) DMSO concentrations; it was found that there is a pronounced selectivity of the resulting water pores to potassium ions as compared to chloride ions, confirming thereby the results of ref 77.

5. Transmembrane Lipid Translocation (Flip-Flop)

5.1. Energetics of Lipid Transmembrane Translocation

As described earlier in section 3.9, Tieleman and Marrink²⁰⁶ calculated the PMF of a lipid in a DPPC bilayer using umbrella sampling by pulling the phosphate group of a lipid through a bilayer and restraining it at different distances across the bilayer. The resulting PMF profile represents the free energy cost of moving a lipid to a specific location from its equilibrium position. The difference in the PMF of a lipid near its equilibrium position and in the middle of the bilayer is found to be around 80 kJ/mol (see Figure 8) and corresponds to the free-energy of translocation of a lipid across a bilayer (lipid flip-flop).²⁰⁶ For a DPPC bilayer, such a transmembrane translocation is accompanied by the formation of a small water pore (when the lipid phosphate group is restrained in the bilayer center), suggesting that the free-energy for pore formation is also around 80 kJ/mol. Assuming that the lipid flip-flop is pore-mediated and taking 10 ns as a typical time for a lipid translocation through a water pore after the pore has been formed, the authors estimated a time scale of lipid translocation to be around 10^5 s or ca. 30 h.²⁰⁶ This time scale is in agreement with experimental values, which scatter from 1 to 90 h depending on experimental conditions.^{4,233}

The calculations of the lipid PMF have recently been systematically extended to a series of phosphatidylcholine bilayers comprised of dilauroyl-phosphatidylcholine (DLPC), DMPC, DPPC, palmitoyl-oleoyl-phosphatidylcholine (POPC), and dioleoyl-phosphatidylcholine (DOPC) lipids.²⁰⁷ The respective PMF profiles presented in Figure 8 clearly demonstrate that the free-energy barrier for lipid translocation increases with the bilayer thickness: the values of 16, 40, 80, 89, and 94 kJ were found for DLPC, DMPC, DPPC, POPC, and DOPC bilayers, respectively.²⁰⁷ As mentioned in section 3.9, the lipid translocation across DLPC, DMPC, and DPPC bilayers is accompanied by the formation of a water pore spanning the entire bilayer. Interestingly, the PMF profiles for DLPC and DMPC bilayers are characterized by the appearance of a plateau near the bilayer center (see Figure 8), which in the case of a DLPC bilayer corresponds to the location where the pore formation occurs. The low free-energy barriers for lipid translocation calculated for DLPC and DMPC bilayers suggest unrealistically fast flip-flop rates for those bilayers, which might point to possible force-field issues.²⁰⁷ For the bilayers comprising unsaturated POPC and DOPC lipids that have longer tails than DLPC, DMPC, and DPPC, pulling a lipid through the bilayer strongly deforms the bilayer and the formation of transient water defects is observed. However, no water pores spanning the entire bilayer are formed in POPC and DOPC bilayers, which

implies that the free-energy barrier of pore formation in these lipids is higher than that of lipid translocation.²⁰⁷

In another recent study by Tieleman et al., they examined the effect of cholesterol on phospholipid transmembrane translocation.²⁰⁸ Cholesterol is an essential component of mammalian plasma membranes, as they contain up to 25–40 mol % of cholesterol. The PMF of a lipid in DPPC bilayers containing 20 and 40 mol % of cholesterol was calculated, and it turned out that the presence of cholesterol increases the free-energy barrier for lipid translocation across the bilayer; the values of 106 and 111 kJ/mol were found for DPPC translocation across DPPC/Chol bilayers with 20 and 40 mol % of cholesterol, respectively.²⁰⁸ These values considerably exceed the 80 kJ/mol reported for a cholesterol-free DPPC bilayer.²⁰⁶ This is an indication that cholesterol makes a phospholipid bilayer more rigid and less prone to deformation. Essentially, no pore formation was found in DPPC bilayers containing cholesterol, indicating that the free-energy barriers of pore formation in DPPC/cholesterol bilayers are higher than the barriers for phospholipid translocation across the bilayer. As for the transmembrane translocation of a cholesterol molecule itself, it is not accompanied by pore formation either.²³⁴

5.2. Pore-Mediated Lipid Translocation (Flip-Flop)

As discussed in the Introduction, there are numerous experimental indications suggesting that migration of lipids from one leaflet of a lipid membrane to another (lipid flip-flop) could be a pore-mediated process. In particular, lipid flip-flop was observed in electroporation experiments that employed both long and submicrosecond pulses.^{235–237} Computational results summarized in the previous section also suggest that lipid translocation across a membrane occurs through transient water pores, at least for sufficiently thin cholesterol-free lipid bilayers.^{206–208}

Taken together, the above findings allow one to formulate one possible molecular mechanism of passive lipid translocation across protein-free lipid membranes: Lipid flip-flop takes place through water pores (defects); that is, the appearance of a transient pore in the membrane inevitably leads to diffusive translocation of lipids through the pore.⁷⁸ This also implies that the formation of water pores in lipid membranes is the rate-limiting step in the process of transmembrane lipid translocation. A number of simulation studies that we survey below indeed confirm this view: Once a water pore is preformed in a membrane, the pore-mediated lipid translocation occurs spontaneously on a time scale of tens of nanoseconds. Remarkably, the particular way by which the pore is preformed is irrelevant for this flip-flop mechanism.

The pore-mediated lipid translocation in atomic-scale resolution was reported for the first time in ref 60, where the spontaneous formation of a small DPPC vesicle in water was studied. Upon aggregation of lipid molecules, a vesicle with several water pores was observed; these pores were found to facilitate the equilibration of the vesicle by the pore-mediated translocation of lipids between the inner and outer leaflets.⁶⁰ The flip-flop events were found to be very fast, as they occurred on a time-scale of 10 ns. Such a short time-scale may be explained by the stress developed between the opposite leaflets upon vesicle formation, speeding up lipid translocation via pores.

A detailed molecular picture of the pore-mediated flip-flop was revealed in ref 78. The authors employed a

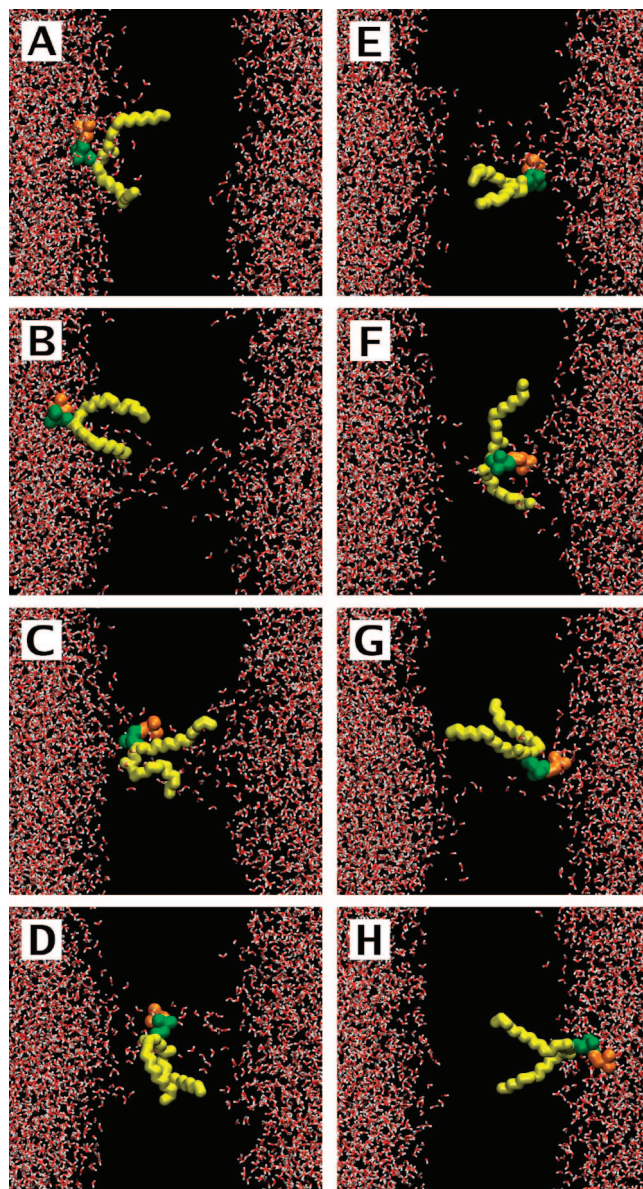


Figure 9. Lipid translocation through a pore induced by a transmembrane ionic charge imbalance: (A) 0 ps; (B) 43.85 ns; (C) 118.9 ns; (D) 122.4 ns; (E) 152.7 ns; (F) 204.65 ns; (G) 208.9 ns; and (H) 215 ns. Only the flip-flopped lipid is shown: its acyl chains are colored in yellow, and choline and phosphate groups are in orange and green, respectively. The rest of the lipids are not shown; water molecules are presented in red and white. Reproduced with permission from ref 78. Copyright 2007 American Chemical Society.

sufficiently high transmembrane imbalance of cations (either sodium or potassium ions) to preform water pores in DMPC lipid bilayers. Under such conditions, the formation of water pores occurred on a nanosecond time scale,^{76–79} followed by pore-mediated leakage of ions (which quickly (within 5–6 ns) discharged the transmembrane ionic charge imbalance) and spontaneous pore-mediated translocation of lipid molecules from one leaflet to another.^{78,80} The overall process of lipid flip-flop through a preformed water pore is visualized in Figure 9. First, a water pore spanning the bilayer is formed (Figure 9B). After some time (about 100 ns in this particular case),⁷⁸ one of the lipids diffuses laterally to the pore site and enters the pore, lining it by its headgroup (Figure 9C). At this point, the spontaneous diffusive translocation of a lipid through the pore started, involving desorption of lipid

hydrocarbon tails out of the leaflet (Figure 9D). Eventually, one finds the appearance of the lipid in the opposite leaflet and the reorientation of the lipid (Figure 9E). The irreversible accommodation of a lipid in the opposite leaflet involves detachment of its headgroup out of the pore “walls” and lateral diffusion of the lipid away from the pore; see Figure 9E–G. This process can be facilitated by pore closure, as seen for the particular flip-flop event (Figure 9H). Overall, based on the analysis of 50 successful flip-flop events in DMPC bilayers with a preformed pore at $T = 323$ K, the average duration of a pore-mediated lipid translocation was found to be around 60 ns. However, flip-flop times for individual lipids scattered considerably from 10 to 130 ns, emphasizing the stochastic nature of pore-mediated lipid flip-flop.⁷⁸

Electric field-induced water pores were also employed in refs 68 and 69 to study the externalization of phosphatidylserine (PS) lipids. The anionic PS lipids are normally located mostly on the inner leaflet of cell membranes. Their appearance on the opposite, outer leaflet (externalization) is associated with programmed cell death.¹⁵ In simulations,^{68,69} an asymmetric PC/PS lipid bilayer with a few PS lipids present in one of the leaflets was exposed to a transmembrane voltage induced either by an external electric field^{68,69} or by a transmembrane ionic charge imbalance.⁶⁹ The authors showed that when the transmembrane voltage was sufficiently high (greater than 450 mV/nm), a transient water pore was formed in the bilayer on a nanosecond time scale and the anionic PS lipid was electrophoretically dragged through the pore.^{68,69} The PS translocation occurred only if the direction of the electric field was such that the negative electrode was on the same side as the anionic PC/PS leaflet. Furthermore, no PS externalization was observed in the absence of a hydrophilic pore spanning the bilayer. The process of the electric field-induced PS externalization was found to be very fast: at an applied voltage of 450 mV/nm, pore formation and subsequent PS translocation took less than 10 ns.⁶⁸ We note that similar findings were reported earlier by Hu et al.,⁷² who employed a coarse-grained model for lipid molecules and an atomistic representation of water molecules.

The water pores induced by the antimicrobial peptides have also been shown to serve as a pathway for transmembrane lipid translocation. In particular, Marrink et al.¹⁵¹ detected such lipid flip-flop through the pores induced by the magainin MG-H2 peptide. The number of lipid translocations observed in the simulations ranged from one to five, with the average flip-flop rate being two per 100 ns. Interestingly, the lipid flip-flop was always initiated on the peptide-enriched leaflet and ended up on the opposite, peptide-free leaflet.¹⁵¹

As the formation of water pores in lipid membranes can be induced by surface-active molecules, one can also expect transmembrane lipid translocations in such systems. This was indeed the case for a series of phosphatidylcholine bilayers in aqueous solution with dimethylsulfoxide (DMSO).²³⁸ Three single-component bilayers comprised of DMPC, DPPC, and POPC lipids were studied at DMSO concentrations that induced formation of transient water pores in the bilayers. Based on 200 lipid translocations resolved in atomic detail, it was concluded that the overall molecular picture of pore-mediated lipid flip-flop stays unchanged compared to the case of the pores induced by other means. However, amphiphilic DMSO molecules, being incorporated in the lipid/water interface, considerably reduced the energy barrier

for lipid desorption and therefore speed up transmembrane lipid translocation.²³⁸ In particular, the characteristic flip-flop time for a DMPC bilayer with DMSO drops to 17 ns as compared to 60 ns reported for DMSO-free DMPC bilayers with preformed pores.⁷⁸ Furthermore, a clear effect of the acyl chain length on the translocation rate was observed: the flip-flop time in the DPPC/DMSO bilayer system (which is characterized by longer acyl chains than those of its DMPC counterpart) was found to be around 25 ns (versus 17 ns for DMPC bilayers). As pore-mediated lipid translocation is driven by thermal fluctuations, temperature also matters: elevating the temperature in the DPPC/DMSO bilayer system from 323 to 350 K was shown to reduce the flip-flop time from 25 to 13 ns.⁷⁸

The occurrence of transmembrane lipid translocation has also been observed in DPPC bilayers with a relatively low concentration of butanol (0.55 M).¹⁴⁰ The corresponding mechanism is most likely linked to the formation of a transient water defect when an alcohol crosses the interior of the membrane. This was shown to be a two-step process.¹⁴⁰ First, one observes the formation of a gap (defect) near the lipid when a neighboring butanol molecule adsorbed by the membrane departs toward the opposite leaflet. Then, this defect makes it possible for the lipid to move to the bilayer center, where it spends around half a nanosecond and eventually jumps to the opposite leaflet.¹⁴⁰ Translocation of lipid molecules was also witnessed in the study of phospholipid bilayers in the presence of ethanol.¹⁴³ When the ethanol concentration exceeded 12 mol % (lipid-free basis), the formation of nonbilayer micelle-like structures in the membrane interior was observed. The lipids involved in such micelle-like structures turn out to belong to both leaflets, so that one can find an extensive mixing of lipids from the opposite leaflets of the original bilayer.¹⁴³

Pore-facilitated lipid flip-flop has recently been employed for the equilibration of lipid vesicles.^{204,205} Risselada et al. used the coarse-grained MARTINI force-field for phospholipids and studied aggregation of a random mixture of lipids and water into a vesicle.^{204,205} After initial self-assembly, the transmonolayer lipid distribution in such vesicles was still unequilibrated. Further equilibration was achieved by insertion of artificial hydrophilic pores into a vesicle: the pores provide a way by which the inner and outer leaflet can exchange lipids. The authors^{204,205} kept such pores open by applying a cylindrical potential, similar to the approach originally developed in refs 195 and 197. It was shown that vesicles with artificial pores can be equilibrated within approximately 300 ns.²⁰⁵ After that period, pore-mediated lipid translocations still occur but there is no net transport of lipids. For DPPC bilayers the average flip-flop time was found to be 10 ns, 5 ns, and 2.5 ns at 290, 323, and 360 K, respectively.²⁰⁵ Therefore, one can see again the effect of temperature arising from the increased diffusion rate of lipids at higher temperature. Furthermore, the flip-flop times obtained are shorter than those reported for atomic-scale models,^{60,78,238} presumably due to loss of detail in the coarse-grained MARTINI model.

6. Polyelectrolyte Trafficking across Lipid Membranes

We conclude this review with computational studies that have addressed defect-mediated permeation of polyelectrolyte molecules through lipid membranes. This includes trafficking of DNA strands and strongly charged cationic dendrimers.

The interaction of a DNA fragment with an electropermeabilized phospholipid membrane was studied by Tarek.⁶⁷ The problem is highly relevant to the electroporative delivery of genes into cells.²³⁹ In ref 67 a short, 12-basepair DNA duplex was placed near the surface of a palmitoyl-oleoyl-phosphatidylcholine (POPC) lipid bilayer, and an external electric field of 1 V/nm was applied to the system. This strong electric field induced several hydrophilic pores in the bilayer, with one of the pores being created beneath the DNA fragment. The DNA then diffused toward the interior of the bilayer through this pore. Once the DNA duplex migrated inside the bilayer, it came in contact with lipid headgroups lining the hydrophilic walls of the pore, forming a stable DNA/lipid membrane complex.⁶⁷ Interestingly, the applied electric field did not modify the structure of the DNA duplex itself. Note that DNA migration from one side of a membrane to another was beyond the scope of that study.⁶⁷

Interactions of cationic dendrimers with lipid membranes are relevant to the use of these synthetic polymers as nonviral vectors for drug and gene delivery and were discussed in detail in section 3.7. Although existing computational studies have never observed a complete permeation event of a dendrimer across a membrane, they can shed some light on the possible molecular mechanisms behind such trafficking.

As shown in refs 184 and 185, cationic dendrimers of generation five and larger can either disrupt the bilayer structure, which results in pore formation, or considerably deform it, which could potentially lead to wrapping of a dendrimer by the lipid bilayer. The former occurs when the undulation modes of a bilayer are suppressed because a small bilayer patch is being considered¹⁸⁴ (a simulation-specific problem) or because there exists interactions of other dendrimers with the bilayer, creating bilayer regions with positive curvature.¹⁸⁵

If the bilayer structure is disrupted and a transmembrane pore is formed, a dendrimer gets stuck between two membrane leaflets: The position of the dendrimer within the membrane is stabilized by strong electrostatic interactions between the dendrimer's charged moieties and the lipid polar headgroups of the two bilayer leaflets;^{184,185} see snapshot G5-16 in Figure 7. This scenario suggests that pore-mediated transport of a dendrimer across the lipid membrane is rather unlikely. Note that in a certain sense this situation is reminiscent of the electric-field driven formation of a DNA/lipid membrane complex reported in ref 67.

Alternatively, for the dendrimers of high generations, one can expect partial wrapping of a dendrimer by a lipid bilayer without bilayer disruption.¹⁸⁵ Such a wrapping around the adsorbed dendrimer creates a region on the bilayer surface that is characterized by positive curvature and reduced flexibility.¹⁸⁵ If other dendrimers adsorb onto this region, they can disrupt the bilayer structure (see snapshot G7-4c in Figure 7) and complete the bilayer wrapping around the dendrimer in question, thereby promoting the formation of a small lipid vesicle with the dendrimer inside. Therefore, it is possible that highly charged, cationic dendrimers translocate the lipid bilayer along the endocytosis pathway.^{183,240} Further simulation studies are needed to give a definitive answer regarding the molecular mechanism of dendrimer trafficking across cell membranes.

The translocation of macromolecules across membranes is a large-scale process. It involves not only the actual event where the macromolecule crosses the membrane but also the diffusion of the molecule to the vicinity of the membrane.

This implies that translocation is a hydrodynamic process where the interactions mediated by the solvent are also important. While detailed studies of this issue through atomistic models for DNA, RNA, and related molecules have not been published, studies with simplified polymer models have provided useful insight into this matter. Yeomans and her collaborators²⁴¹ compared polymer translocation processes with and without conservation of momentum and found that the conservation of momentum sped up the translocation of a polymer across a pore. Essentially, the momentum conservation gives rise to vortices that push the polymer forward (back-flow) and in this manner promote its translocation rate. From the simulation point of view, this finding is relevant, since many of the current simulation models used for atomistic and coarse-grained modeling of the dynamics of biomolecules and membranes do not conserve momentum. One way to correct this matter would be to implement the dissipative particle dynamics (DPD) thermostat^{242,243} to the simulation engines such as GROMACS and NAMD; the DPD thermostat satisfies momentum conservation and hence can generate the correct hydrodynamic behavior.

More recently, a number of groups have elucidated the translocation phenomena in more detail, with an objective to unravel the physical principles associated with polymer translocation under the influence of an applied external field. While these studies consider translocation through nanopores in general rather than pores in membranes in particular, they provide insight that facilitates further studies in the context of membranes.^{244,245}

7. Conclusions

Defect-mediated trafficking across cell membranes is highly relevant from the point of view of both cell function and numerous practical applications in medicine and biotechnology. On the one hand, unassisted passive transport of solutes via membranes is always present in living cells along with active mechanisms of translocation. On the other hand, controlled modulation of the membrane structure is at the heart of many biomedical applications, as they often imply the interaction of various therapeutic molecules with cell membranes.

Insights into defect-mediated trafficking across cell membranes require atomic resolution, which is still unattainable by most experimental techniques. The required resolution, however, can be attained from molecular simulations, which are now able to reproduce many of the experimental data with confidence and also make predictions for experimental new studies to be done. The past decade has seen an extraordinary contribution from molecular simulations in the field of membrane biophysics, with the impetus being the timely developments in computing power, realistic molecular models, and highly efficient simulation codes. These simulations have provided much needed insights and generic understanding of the mechanisms of formation of transient membrane defects and defect-mediated trafficking at nearly atomic resolution, which have formed the basis of the review.

In this review, we have provided a comprehensive overview of major recent developments relevant to *in silico* modeling of defect-mediated trafficking across biological membranes. These include simulation studies of the formation of transient water defects induced in protein-free lipid membranes by an electric field (electroporation), mechanical stress, shock waves (sonoporation), surface-active molecules,

small cationic peptides, and polyelectrolytes as well as direct atomically resolved observations of defect-mediated translocations of salt ions, lipid molecules, and polyelectrolytes (DNA duplexes and cationic dendrimers) across the membrane. Atomic-scale molecular dynamics simulations have been the primary focus of this paper, although the insight gained via more coarse-grained (near-atomistic) models has also been discussed.

Overall, the power of the state-of-the-art *in silico* methods can be best illustrated by such ground-breaking studies as, for example, simulations of electroporation phenomena, which for the first time provided the molecular-level insight into the mechanism of electroporation as well as a direct confirmation of the long-standing hypothesis that an external electric field can promote formation of transient water pores in membranes.^{65,66} Other remarkable examples include discovery of a novel (disordered) type of a toroidal pore induced by antimicrobial peptides,¹⁵¹ selective permeability of porated protein-free lipid membranes with respect to different salt ions,^{76,77,106} and the defect-mediated mechanism of lipid translocation (flip-flop) across sufficiently thin lipid membranes.^{78,206} The latter is also an excellent illustration of how biased MD simulations of a microscopic bilayer system can give access to macroscopic properties of lipid membranes such as the flip-flop rate.²⁰⁶

As for further developments in this area, one can anticipate attempts to model the complete translocation event for various solutes (alone or within a nanocontainer) across biological membranes which would be of considerable importance for many biomedical applications (drug and gene delivery, interactions of cells with nanoparticles, etc). Coupling atomistic MD simulations of membranes with cell-level numerical models will be an important direction of future research for developing new ways to deal with electroporation phenomena. This objective is related to the current interest to bridge atomistic simulations with computational systems biology.²⁴⁶ Furthermore, future electroporation studies need to address an issue related to the mean pore lifetimes observed in simulations and experiments: when the transmembrane electric field is switched off, the pores studied in simulations close in tens of nanoseconds while in experiments this process occurs in several milliseconds.²⁴⁷ It is also interesting to get additional insight into so-called molecular electroporation¹⁵⁶ phenomena, where a highly charged object near a membrane surface can induce a porating electric field similar to conventional electroporation. The composition of model membranes themselves in simulations of defect-mediated solute transport will become more complex in attempts to match the physiological situation more closely. This could imply, for example, incorporating cholesterol into a phospholipid bilayer as well as accounting for an asymmetric transmembrane distribution of lipids⁵⁴ typical of most living cells. In addition, further development and refinement of force-fields is needed to make lipid force-fields compatible with the force-fields of peptides, DNA, and polymers. Accounting for polarizability is another long-standing issue.²⁴⁸ As for coarse-grained models, their applicability to transmembrane solute transport is still rather limited, especially for the bilayer systems in which electrostatics play a role in the formation of water defects. This is mostly due to a uniform dielectric medium employed in most coarse-grained models. The situation could be improved, for example, by making the coarse-grained water particle dipolar.²⁴⁹ Further desired improvements would include, for

example, the implementation of the dissipative particle dynamics thermostat for the most common simulation engines, allowing large-scale studies of dynamic phenomena with realistic hydrodynamics.

8. Acknowledgments

The authors are thankful to Siewert-Jan Marrink, D. Peter Tieleman, P. Thomas Vernier, James C. Weaver, Erik Lindahl, Ronald G. Larson, Hwankyoo Lee, Kenichiro Koshiyama, Wim Briels, Wouter den Otter, Lev Sarkisov, Mark S. P. Sansom, Mark Banaszak Holl, Peter C. Jordan, Gregory A. Voth, Roland Faller, and Erick J. Dufourc for their help during preparation of the review. Funding from the Russian Foundation of Basic Research through Grant No. 08-03-00150 (A.A.G.) and from the Academy of Finland (I.V.) is gratefully acknowledged.

9. References

- (1) Luckey, M. *Membrane Structural Biology*; University Cambridge Press: Cambridge, 2008.
- (2) Voet, D.; Voet, J. G. *Biochemistry*, 3rd ed.; John Wiley & Sons: New York, 2004.
- (3) Iacovache, I.; van der Goot, F. G.; Pernot, L. *Biochim. Biophys. Acta* **2008**, *1778*, 1611.
- (4) Kornberg, R. D.; McConnell, H. M. *Biochemistry* **1971**, *10*, 1111.
- (5) Toyoshima, Y.; Thompson, T. E. *Biochemistry* **1975**, *14*, 1525.
- (6) Deamer, D. W.; Bramhall, J. *Chem. Phys. Lipids* **1986**, *40*, 167.
- (7) Lawaczeck, R. *Ber. Bunsen-Ges. Phys. Chem.* **1998**, *92*, 961.
- (8) Jansen, M.; Blume, A. *Biophys. J.* **1995**, *68*, 997.
- (9) Paula, S.; Volkov, A. G.; VanHoek, A. N.; Haines, T. H.; Deamer, D. W. *Biophys. J.* **1996**, *70*, 339.
- (10) Bordi, F.; Cametti, C.; Motta, A. *J. Phys. Chem. B* **2000**, *104*, 5318.
- (11) Gennis, R. B. *Biomembranes: Molecular Structure and Function*; Springer-Verlag: New York, 1989.
- (12) Zachowski, A. *Biochem. J.* **1993**, *294*, 1.
- (13) Manno, S.; Takakuwa, Y.; Mohandas, N. *Proc. Natl. Acad. Sci. U.S.A.* **2002**, *99*, 1943.
- (14) Pomorski, T.; Hrafnisdottir, S.; Devaux, P. F.; van Meer, G. *Semin. Cell Dev. Biol.* **2001**, *12*, 139.
- (15) Balasubramanian, K.; Schroit, A. *J. Annu. Rev. Physiol.* **2003**, *65*, 701.
- (16) Fadok, V. A.; Voelker, D. R.; Campbell, P. A.; Cohen, J. J.; Bratton, D. L.; Henson, P. M. *J. Immunol.* **1992**, *148*, 2207.
- (17) Bevers, E. M.; Comfurius, P.; Dekkers, D. W. C.; Zwaal, R. F. A. *Biochim. Biophys. Acta* **1999**, *1439*, 317.
- (18) Pomorski, T.; Menon, A. K. *Cell. Mol. Life Sci.* **2006**, *63*, 2908.
- (19) Riggers, R. J.; Pomorski, T.; Holthuis, J. C. M.; Kälin, N.; van Meer, G. *Traffic* **2000**, *1*, 226.
- (20) Marti, J.; Csajka, F. S. *Europhys. Lett.* **2003**, *61*, 409.
- (21) Marti, J.; Csajka, F. S. *Phys. Rev. E* **2004**, *69*, 061918.
- (22) Schwarz, S.; Haest, C. W. M.; Deuticke, B. *Biochim. Biophys. Acta* **1999**, *1421*, 361.
- (23) Anchordoguy, T. J.; Carpenter, J. F.; Crowe, J. H.; Crowe, L. M. *Biochim. Biophys. Acta* **1992**, *1104*, 117.
- (24) Weaver, J. C. *J. Cell. Biochem.* **1993**, *51*, 426.
- (25) Tachibana, K.; Uchida, T.; Ogawa, K.; Yamashita, N.; Tamura, K. *Lancet* **1999**, *353*, 1409.
- (26) Boon, J. M.; Smith, B. D. *Med. Res. Rev.* **2002**, *22*, 251.
- (27) Tieleman, D. P.; Marrink, S. J.; Berendsen, H. J. C. *Biochim. Biophys. Acta* **1997**, *1331*, 235.
- (28) Feller, S. E. *Curr. Opin. Colloid Interface Sci.* **2000**, *5*, 217.
- (29) Scott, H. L. *Curr. Opin. Struct. Biol.* **2002**, *12*, 495.
- (30) Marrink, S. J.; de Vries, A. H.; Tieleman, D. P. *Biochim. Biophys. Acta* **2009**, *1788*, 149.
- (31) Bjelkmar, P.; Niemela, P. S.; Vattulainen, I.; Lindahl, E. *PLoS Comput. Biol.* **2009**, *5*, e1000289.
- (32) Arkin, I. T.; Xu, H.; Jensen, M. O.; Arbely, E.; Bennett, E. R.; Bowers, K. J.; Chow, E.; Dror, R. O.; Eastwood, M. P.; Flitman-Tene, R.; Gregersen, B. A.; Klepeis, J. L.; Kolossvary, I.; Shan, Y.; Shaw, D. E. *Science* **2007**, *317*, 799.
- (33) Ash, W. L.; Zlomislic, M. R.; Oloo, E. O.; Tieleman, D. P. *Biochim. Biophys. Acta* **2004**, *1666*, 158.
- (34) Gumbart, J.; Wang, Y.; Aksimentiev, A.; Tajkhorshid, E.; Schulten, K. *Curr. Opin. Struct. Biol.* **2005**, *15*, 423.
- (35) Lindahl, E.; Sansom, M. S. P. *Curr. Opin. Struct. Biol.* **2008**, *18*, 425.

- (36) Feller, S. E.; MacKerell, A. D. *J. Phys. Chem. B* **2000**, *104*, 7510.
- (37) Feller, S. E.; Gawrisch, K.; MacKerell, A. D. *J. Am. Chem. Soc.* **2002**, *124*, 318.
- (38) Berger, O.; Edholm, O.; Jahnig, F. *Biophys. J.* **1997**, *72*, 2002.
- (39) Sonne, J.; Jensen, M. O.; Hansen, F. Y.; Hemmingsen, L.; Peters, G. H. *Biophys. J.* **2007**, *92*, 4157.
- (40) Klauda, J. B.; Venable, R. M.; Freites, J. A.; O'Connor, J. W.; Tobias, D. J.; Mondragon-Ramirez, C.; Vorobyov, I.; MacKerell, A. D.; Pastor, R. W. *J. Phys. Chem. B* **2010**, *114*, 7830.
- (41) Shelley, J. C.; Shelley, M. Y.; Reeder, R. C.; Bandyopadhyay, S.; Klein, M. L. *J. Phys. Chem. B* **2001**, *105*, 4464.
- (42) Izvekov, S.; Voth, G. A. *J. Phys. Chem. B* **2005**, *109*, 2469.
- (43) Marrink, S. J.; de Vries, A. H.; Mark, A. E. *J. Phys. Chem. B* **2004**, *108*, 750.
- (44) Marrink, S. J.; Risselada, H. J.; Yefimov, S.; Tieleman, D. P.; de Vries, A. H. *J. Phys. Chem. B* **2007**, *111*, 7812.
- (45) Monticelli, L.; Kandasamy, S. K.; Periole, X.; Larson, R. G.; Tieleman, D. P.; Marrink, S. J. *J. Chem. Theor. Comput.* **2008**, *4*, 819.
- (46) Cascales, J. J. L.; de la Torre, J. G.; Marrink, S. J.; Berendsen, H. J. C. *J. Chem. Phys.* **1996**, *104*, 2713.
- (47) Pandit, S. A.; Berkowitz, M. L. *Biophys. J.* **2002**, *82*, 1818.
- (48) Mukhopadhyay, P.; Monticelli, L.; Tieleman, D. P. *Biophys. J.* **2004**, *86*, 1601.
- (49) Gurtovenko, A. A.; Patra, M.; Karttunen, M.; Vattulainen, I. *Biophys. J.* **2004**, *86*, 3461.
- (50) Pandit, S. A.; Jakobsson, E.; Scott, H. L. *Biophys. J.* **2004**, *87*, 3312.
- (51) Aittoniemi, J.; Niemela, P. S.; Hyvonen, M. T.; Karttunen, M.; Vattulainen, I. *Biophys. J.* **2007**, *92*, 1125.
- (52) Niemela, P. S.; Ollila, S.; Hyvonen, M. T.; Karttunen, M.; Vattulainen, I. *PLoS Comput. Biol.* **2007**, *3*, 304.
- (53) Niemela, P. S.; Hyvonen, M. T.; Vattulainen, I. *Biochim. Biophys. Acta* **2009**, *1788*, 122.
- (54) Gurtovenko, A. A.; Vattulainen, I. *J. Am. Chem. Soc.* **2007**, *129*, 5358.
- (55) Gurtovenko, A. A.; Vattulainen, I. *J. Phys. Chem. B* **2009**, *113*, 7194.
- (56) Gurtovenko, A. A.; Vattulainen, I. *J. Phys. Chem. B* **2008**, *112*, 14629.
- (57) Cascales, J. J. L.; Otero, T. F.; Smith, B. D.; Gonzalez, C.; Marquez, M. *J. Phys. Chem. B* **2006**, *110*, 2358.
- (58) Vacha, R.; Berkowitz, M. L.; Jungwirth, P. *Biophys. J.* **2009**, *96*, 4493.
- (59) Marrink, S. J.; Lindahl, E.; Edholm, O.; Mark, A. E. *J. Am. Chem. Soc.* **2001**, *123*, 8638.
- (60) de Vries, A. H.; Mark, A. E.; Marrink, S. J. *J. Am. Chem. Soc.* **2004**, *126*, 4488.
- (61) Marrink, S. J.; Mark, A. E. *J. Am. Chem. Soc.* **2003**, *125*, 15233.
- (62) Frey, W.; White, J. A.; Price, R. O.; Blackmore, P. F.; Joshi, R. P.; Nuccitelli, R.; Beebe, S. J.; Schoenbach, K. H.; Kolb, J. F. *Biophys. J.* **2006**, *90*, 3608.
- (63) Gowrishankar, T. R.; Esser, A. T.; Vasilkoski, Z.; Smith, K. C.; Weaver, J. C. *Biochem. Biophys. Res. Commun.* **2006**, *341*, 1266.
- (64) Weaver, J. C. *IEEE Trans. Dielectr. Electr. Insul.* **2003**, *10*, 754.
- (65) Tieleman, D. P.; Leontiadou, H.; Mark, A. E.; Marrink, S.-J. *J. Am. Chem. Soc.* **2003**, *125*, 6382.
- (66) Tieleman, D. P. *BMC Biochem.* **2004**, *5*, 10.
- (67) Tarek, M. *Biophys. J.* **2005**, *88*, 4045.
- (68) Vernier, P. T.; Ziegler, M. J.; Sun, Y.; Chang, W. V.; Gundersen, M. A.; Tieleman, D. P. *J. Am. Chem. Soc.* **2006**, *128*, 6288.
- (69) Vernier, P. T.; Ziegler, M. J.; Sun, Y.; Gundersen, M. A.; Tieleman, D. P. *Phys. Biol.* **2006**, *3*, 233.
- (70) Vernier, P. T.; Ziegler, M. J. *J. Phys. Chem. B* **2007**, *111*, 12993.
- (71) Ziegler, M. J.; Vernier, P. T. *J. Phys. Chem. B* **2008**, *112*, 13588.
- (72) Hu, Q.; Joshi, R. P.; Schoenbach, K. H. *Phys. Rev. E* **2005**, *72*, 031902.
- (73) Hu, Q.; Viswanadham, S.; Joshi, R. P.; Schoenbach, K. H.; Beebe, S. J.; Blackmore, P. F. *Phys. Rev. E* **2005**, *71*, 031914.
- (74) Böckmann, R. A.; de Groot, B. L.; Kakorin, S.; Neumann, E.; Grubmüller, H. *Biophys. J.* **2008**, *95*, 1837.
- (75) Roux, B. *Biophys. J.* **2008**, *95*, 4205.
- (76) Gurtovenko, A. A.; Vattulainen, I. *J. Am. Chem. Soc.* **2005**, *127*, 17570.
- (77) Gurtovenko, A. A.; Vattulainen, I. *Biophys. J.* **2007**, *92*, 1878.
- (78) Gurtovenko, A. A.; Vattulainen, I. *J. Phys. Chem. B* **2007**, *111*, 13554.
- (79) Gurtovenko, A. A.; Vattulainen, I. In *Biomembrane Frontiers: Nanostructures, Models, and the Design of Life. Handbook of Modern Biophysics*; Faller, R., Longo, M. L., Risbud, S. H., Jue, T., Eds.; Humana Press: Dordrecht, 2009; p 121.
- (80) Kandasamy, S. K.; Larson, R. G. *J. Chem. Phys.* **2006**, *125*, 074901.
- (81) Sachs, J. N.; Crozier, P. S.; Woolf, T. B. *J. Chem. Phys.* **2004**, *121*, 10847.
- (82) Gurtovenko, A. A. *J. Chem. Phys.* **2005**, *122*, 244902.
- (83) Delemotte, L.; Dehez, F.; Treptow, W.; Tarek, M. *J. Phys. Chem. B* **2008**, *112*, 5547.
- (84) Herrera, F. E.; Pantano, S. *J. Chem. Phys.* **2009**, *130*, 195105.
- (85) Bostick, D.; Berkowitz, M. L. *Biophys. J.* **2003**, *85*, 91.
- (86) Gurtovenko, A. A.; Vattulainen, I. *J. Chem. Phys.* **2009**, *130*, 215107.
- (87) Glaser, R. W.; Leikin, S. L.; Chernomordik, L. V.; Pastushenko, V. F.; Sokirko, A. I. *Biochim. Biophys. Acta* **1988**, *940*, 275.
- (88) Griese, T.; Kakorin, S.; Neumann, E. *Phys. Chem. Chem. Phys.* **2002**, *4*, 1217.
- (89) Abiror, I. G.; Arakelyan, V. B.; Chernomordik, L. V.; Chizmadzhev, Y. A.; Pastushenko, V. F.; Tarasevich, M. R. *Bioelectrochem. Bioenerg.* **1979**, *6*, 37.
- (90) Siu, S. W. I.; Böckmann, R. A. *J. Struct. Biol.* **2007**, *157*, 545.
- (91) Kakorin, S.; Brinkman, U.; Neumann, E. *Biophys. Chem.* **2005**, *117*, 155.
- (92) van Uiterit, I.; Gac, S. L.; van der Berg, A. *Biochim. Biophys. Acta* **2010**, *1798*, 21.
- (93) Vernier, P. T.; Levine, Z. A.; Wu, Y. H.; Joubert, V.; Ziegler, M. J.; Mir, L. M.; Tieleman, D. P. *PLoS One* **2009**, *4*, e7966.
- (94) Wong-Ekkabut, J.; Xu, Z. T.; Triampo, W.; Tang, I. M.; Tieleman, D. P.; Monticelli, L. *Biophys. J.* **2007**, *93*, 4225.
- (95) DeBruin, K. A.; Krassowska, W. *Biophys. J.* **1999**, *77*, 1213.
- (96) DeBruin, K. A.; Krassowska, W. *Biophys. J.* **1999**, *77*, 1225.
- (97) Stewart, D. A.; Gowrishankar, T. R.; Weaver, J. C. *IEEE Trans. Plasma Sci.* **2004**, *32*, 1696.
- (98) Vasilkoski, Z.; Esser, A. T.; Gowrishankar, T. R.; Weaver, J. C. *Phys. Rev. E* **2006**, *74*, 021904.
- (99) Krassowska, W.; Filev, P. D. *Biophys. J.* **2007**, *92*, 404.
- (100) Smith, K. C.; Weaver, J. C. *Biophys. J.* **2008**, *95*, 1547.
- (101) Zhelev, D. V.; Needham, D. *Biochim. Biophys. Acta* **1993**, *1147*, 89.
- (102) Sandre, O.; Moreaux, L.; Brochard-Wyart, F. *Proc. Natl. Acad. Sci. U.S.A.* **1999**, *96*, 10591.
- (103) Olbrich, K.; Rawicz, W.; Needham, D.; Evans, E. *Biophys. J.* **2000**, *79*, 321.
- (104) Leontiadou, H.; Mark, A. E.; Marrink, S.-J. *Biophys. J.* **2004**, *86*, 2156.
- (105) Knecht, V.; Muller, M.; Bonn, M.; Marrink, S. J.; Mark, A. E. *J. Chem. Phys.* **2005**, *122*, 024704.
- (106) Leontiadou, H.; Mark, A. E.; Marrink, S.-J. *Biophys. J.* **2007**, *92*, 4209.
- (107) Evans, E.; Heinrich, V. C. *R. Phys.* **2003**, *4*, 265.
- (108) Tolpekina, T. V.; den Otter, W. K.; Briels, W. J. *J. Chem. Phys.* **2004**, *121*, 8014.
- (109) Barnett, A.; Weaver, J. C. *Bioelectrochem. Bioenerg.* **1991**, *25*, 163.
- (110) Patra, M.; Karttunen, M.; Hyvönen, M. T.; Falck, E.; Lindqvist, P.; Vattulainen, I. *Biophys. J.* **2003**, *84*, 3636.
- (111) Anézo, C.; de Vries, A. H.; Hóltje, H. D.; Tieleman, D. P.; Marrink, S. J. *J. Phys. Chem. B* **2003**, *107*, 9424.
- (112) Patra, M.; Karttunen, M.; Hyvönen, M. T.; Falck, E.; Vattulainen, I. *J. Phys. Chem. B* **2004**, *108*, 4485.
- (113) Böckmann, R. A.; Hac, A.; Heimburg, T.; Grubmüller, H. *Biophys. J.* **2003**, *85*, 1647.
- (114) Pandit, S. A.; Bostick, D.; Berkowitz, M. L. *Biophys. J.* **2003**, *84*, 3743.
- (115) Gurtovenko, A. A.; Vattulainen, I. *J. Phys. Chem. B* **2008**, *112*, 1953.
- (116) Böckmann, R. A.; Grubmüller, H. *Angew. Chem., Int. Ed.* **2004**, *43*, 1021.
- (117) Kodama, T.; Doukas, A. G.; Hamblin, M. R. *Biochim. Biophys. Acta* **2002**, *1542*, 186.
- (118) Rosenthal, I.; Sostaric, J. Z.; Riesz, P. *Ultrason. Sonochem.* **2004**, *11*, 349.
- (119) Brayman, A. A.; Coppage, M. L.; Vaidya, S.; Miller, M. W. *Ultrasound Med. Biol.* **1999**, *25*, 999.
- (120) Feril, L. B.; Kondo, T.; Umemura, S.; Tachibana, K.; Manalo, A. H.; Riesz, P. *J. Med. Ultrason.* **2002**, *29*, 173.
- (121) Koshiyama, K.; Kodama, T.; Yano, T.; Fujikawa, S. *Biophys. J.* **2006**, *91*, 2198.
- (122) Koshiyama, K.; Kodama, T.; Yano, T.; Fujikawa, S. In *AIP Conference Proceedings: Therapeutic Ultrasound*; Clement, G. T., McDannold, N. J., Hynynen, K., Eds.; 2006; Vol. 829, p 583.
- (123) Koshiyama, K.; Kodama, T.; Fujikawa, T. Y. S. *Biochim. Biophys. Acta* **2008**, *1778*, 1423.
- (124) Rall, W. F.; Fahy, G. M. *Nature* **1985**, *313*, 573.
- (125) Ahkong, Q. F.; Fisher, D.; Tampion, W.; Lucy, J. A. *Nature* **1975**, *253*, 194.
- (126) Yu, Z.-W.; Quinn, P. J. *Biophys. Chem.* **1998**, *70*, 35.
- (127) Williams, A. C.; Barry, B. W. *Adv. Drug Delivery Rev.* **2004**, *56*, 603.
- (128) Gurtovenko, A. A.; Anwar, J. J. *J. Phys. Chem. B* **2007**, *111*, 10453.
- (129) Notman, R.; Noro, M.; O'Malley, B.; Anwar, J. J. *J. Am. Chem. Soc.* **2006**, *128*, 13982.
- (130) Sum, A. K.; de Pablo, J. *Biophys. J.* **2003**, *85*, 3636.
- (131) Holte, L. L.; Gawrisch, K. *Biochemistry* **1997**, *36*, 4669.

- (132) Feller, S. E.; Brown, C. A.; Nizza, D. T.; Gawrisch, K. *Biophys. J.* **2002**, *82*, 1396.
- (133) Barry, J. A.; Gawrisch, K. *Biochemistry* **1994**, *33*, 8082.
- (134) Vierl, U.; Lobbecke, L.; Nagel, N.; Cevc, G. *Biophys. J.* **1994**, *67*, 1067.
- (135) Ly, H. V.; Longo, M. L. *Langmuir* **2002**, *18*, 8988.
- (136) Ly, H. V.; Longo, M. L. *Biophys. J.* **2004**, *87*, 1013.
- (137) Patra, M.; Salonen, E.; Terama, E.; Vattulainen, I.; Faller, R.; Lee, B. W.; Holopainen, J.; Karttunen, M. *Biophys. J.* **2006**, *90*, 1121.
- (138) Chanda, J.; Bandyopadhyay, S. *Langmuir* **2006**, *22*, 3775.
- (139) Chanda, J.; Chakraborty, S.; Bandyopadhyay, S. *J. Phys. Chem. B* **2006**, *110*, 3791.
- (140) Dickey, A. N.; Faller, R. *Biophys. J.* **2007**, *92*, 2366.
- (141) Griepernau, B.; Leis, S.; Schneider, M. F.; Sikor, M.; Steppich, D.; Bockmann, R. A. *Biochim. Biophys. Acta* **2007**, *1768*, 2899.
- (142) Terama, E.; Ollila, O. H. S.; Salonen, E.; Rowat, A. C.; Trandum, C.; Westh, P.; Patra, M.; Karttunen, M.; Vattulainen, I. *J. Phys. Chem. B* **2008**, *112*, 4131.
- (143) Gurtovenko, A. A.; Anwar, J. J. *J. Phys. Chem. B* **2009**, *113*, 1983.
- (144) Mou, J.; Yang, J.; Huang, C.; Shao, Z. *Biochemistry* **1994**, *33*, 9981.
- (145) Isomaa, B.; Hagerstrand, H.; Paatero, G. *Biochim. Biophys. Acta* **1987**, *899*, 93.
- (146) Galarneau, A.; Sartori, F.; Cangiotti, M.; Mineva, T.; Di Renzo, F.; Ottaviani, M. F. *J. Phys. Chem. B* **2010**, *114*, 2140.
- (147) Siwko, M. E.; de Vries, A. H.; Mark, A. E.; Kozubek, A.; Marrink, S. J. *Biophys. J.* **2009**, *96*, 3140.
- (148) Esteban-Martin, S.; Risselada, H. J.; Salgado, J.; Marrink, S. J. *J. Am. Chem. Soc.* **2009**, *131*, 15194.
- (149) Zasloff, M. *Nature* **2002**, *415*, 389.
- (150) Brogden, K. A. *Nature Rev. Microbiol.* **2005**, *3*, 238.
- (151) Leontiadou, H.; Mark, A. E.; Marrink, S.-J. *J. Am. Chem. Soc.* **2006**, *128*, 12156.
- (152) Ludtke, S. J.; He, K.; Heller, W. T.; Harroun, T. A.; Yang, L.; Huang, H. W. *Biochemistry* **1996**, *35*, 13723.
- (153) Matsuzaki, K.; Murase, O.; Fujii, N.; Miyajima, K. *Biochemistry* **1996**, *35*, 11361.
- (154) Sengupta, D.; Leontiadou, H.; Mark, A. E.; Marrink, S. J. *Biochim. Biophys. Acta* **2008**, *1778*, 2308.
- (155) Jean-Francois, F.; Elezgaray, J.; Berson, P.; Vacher, P.; Dufourc, E. J. *Biophys. J.* **2008**, *95*, 5748.
- (156) Miteva, M.; Andersson, M.; Karshikoff, A.; Otting, G. *FEBS Lett.* **1999**, *462*, 155.
- (157) Binder, H.; Lindblom, G. *Biophys. J.* **2003**, *85*, 982.
- (158) Zorko, M.; Langel, U. *Adv. Drug Delivery Rev.* **2005**, *57*, 529.
- (159) El-Andaloussi, S.; Langel, T. H. U. *Curr. Pharm. Des.* **2005**, *11*, 3597.
- (160) Brooks, H.; Lebleu, B.; Vives, E. *Adv. Drug Delivery Rev.* **2005**, *57*, 559.
- (161) Yesylevskyy, S.; Marrink, S. J.; Mark, A. E. *Biophys. J.* **2009**, *97*, 40.
- (162) Herce, H. D.; Garcia, A. E. *Proc. Natl. Acad. Sci. U.S.A.* **2007**, *104*, 20805.
- (163) Herce, H. D.; Garcia, A. E.; Litt, J.; Kane, R. S.; Martin, P.; Enrique, N.; Rebolledo, A.; Milesi, V. *Biophys. J.* **2009**, *97*, 1917.
- (164) Rzepiela, A. J.; Sengupta, D.; Goga, N.; Marrink, S. J. *Faraday Discuss.* **2010**, *144*, 431.
- (165) Vorobyov, I.; Li, L.; Allen, T. W. *J. Phys. Chem. B* **2008**, *112*, 9588.
- (166) Bond, P. J.; Parton, D. L.; Clark, J. F.; Sansom, M. S. P. *Biophys. J.* **2008**, *95*, 3802.
- (167) Thogersen, L.; Schiott, B.; Vosegaard, T.; Nielsen, N. C.; Tajkhorshid, E. *Biophys. J.* **2008**, *95*, 4337.
- (168) Gkeka, P.; Sarkisov, L. *J. Phys. Chem. B* **2009**, *113*, 6.
- (169) Gkeka, P.; Sarkisov, L. *J. Phys. Chem. B* **2010**, *114*, 826.
- (170) Hong, S. P.; Leroueil, P. R.; Janus, E. K.; Peters, J. L.; Kober, M. M.; Islam, M. T.; Orr, B. G.; Baker, J. R.; Holl, M. M. B. *Bioconjugate Chem.* **2006**, *17*, 728.
- (171) Leroueil, P. R.; Berry, S. A.; Duthie, K.; Han, G.; Rotello, V. M.; McNerny, D. Q.; Baker, J. R.; Orr, B. G.; Holl, M. M. B. *Nano Lett.* **2008**, *8*, 420.
- (172) Frechet, J. M. J. *Science* **1994**, *263*, 1710.
- (173) van Duijvenbode, R. C.; Borkovec, M.; Koper, G. J. M. *Polymer* **1998**, *39*, 2657.
- (174) KukowskaLatallo, J. F.; Bielinska, A. U.; Johnson, J.; Spindler, R.; Tomalia, D. A.; Baker, J. *Proc. Natl. Acad. Sci. U.S.A.* **1996**, *93*, 4897.
- (175) Esfand, R.; Tomalia, D. A. *Drug Discov. Today* **2001**, *6*, 427.
- (176) Dufes, C.; Uchegbu, I. F.; Schatzlein, A. G. *Adv. Drug. Delivery Rev.* **2005**, *57*, 2177.
- (177) Svenson, S.; Tomalia, D. A. *Adv. Drug. Delivery Rev.* **2005**, *57*, 2106.
- (178) Malik, N.; Evagorou, E. G.; Duncan, R. *Anti-Cancer Drugs* **1999**, *10*, 767.
- (179) Mecke, A.; Lee, I.; Baker, J. R.; Holl, M. M. B.; Orr, B. G. *Eur. Phys. J. E* **2004**, *14*, 7.
- (180) Voulgarakis, N. K.; Rasmussen, K. O.; Welch, P. M. *J. Chem. Phys.* **2009**, *130*, 155101.
- (181) Kelly, C. V.; Leroueil, P. R.; Nett, E. K.; Wereszczynski, J. M.; Baker, J. R.; Orr, B. G.; Holl, M. M. B.; Andricioaei, I. *J. Phys. Chem. B* **2008**, *112*, 9337.
- (182) Kelly, C. V.; Leroueil, P. R.; Orr, B. G.; Holl, M. M. B.; Andricioaei, I. *J. Phys. Chem. B* **2008**, *112*, 9346.
- (183) Kelly, C. V.; Liroff, M. G.; Triplett, L. D.; Leroueil, P. R.; Mullen, D. G.; Wallace, J. M.; Meshinchi, S.; Baker, J. R.; Orr, B. G.; Holl, M. M. B. *ACS Nano* **2009**, *3*, 1886.
- (184) Lee, H.; Larson, R. G. *J. Phys. Chem. B* **2006**, *110*, 18204.
- (185) Lee, H.; Larson, R. G. *J. Phys. Chem. B* **2008**, *112*, 7778.
- (186) Lee, H.; Larson, R. G. *J. Phys. Chem. B* **2008**, *112*, 12279.
- (187) Lee, H.; Larson, R. G. *Molecules* **2009**, *14*, 423.
- (188) Yan, L. T.; Yu, X. B. *Macromolecules* **2009**, *42*, 6277.
- (189) Yan, L. T.; Yu, X. B. *ACS Nano* **2009**, *3*, 2171.
- (190) Sohal, R. S.; Weindruch, R. *Science* **1996**, *273*, 59.
- (191) Chatterjee, S. N.; Agarwal, S. *Free Radical Biol. Med.* **1988**, *4*, 51.
- (192) Litster, J. D. *Phys. Lett. A* **1975**, *53*, 193.
- (193) Taupin, C.; Dvolaitzky, M.; Sauterey, C. *Biochemistry*. **1975**, *14*, 4771.
- (194) Farago, O.; Santangelo, C. D. *J. Chem. Phys.* **2005**, *122*, 044901.
- (195) Tolpekina, T. V.; den Otter, W. K.; Briels, W. J. *J. Chem. Phys.* **2004**, *121*, 12060.
- (196) den Otter, W. K. *J. Chem. Phys.* **2009**, *131*, 205101.
- (197) Wohler, J.; den Otter, W. K.; Edholm, O.; Briels, W. J. *J. Chem. Phys.* **2006**, *124*, 154905.
- (198) Notman, R.; Anwar, J.; Briels, W. J.; Noro, M. G.; den Otter, W. K. *Biophys. J.* **2008**, *95*, 4763.
- (199) Beckstein, O.; Biggin, P. C.; Sansom, M. S. P. *J. Phys. Chem. B* **2001**, *105*, 12902.
- (200) Beckstein, O.; Sansom, M. S. P. *Proc. Natl. Acad. Sci. U.S.A.* **2003**, *100*, 7063.
- (201) Allen, R.; Melchionna, S.; Hansen, J. P. *Phys. Rev. Lett.* **2002**, *89*, 175502.
- (202) Allen, R.; Hansen, J. P.; Melchionna, S. *J. Chem. Phys.* **2003**, *119*, 3905.
- (203) Notman, R.; den Otter, W. K.; Noro, M. G.; Briels, W. J.; Anwar, J. *Biophys. J.* **2007**, *93*, 2056.
- (204) Risselada, H. J.; Mark, A. E.; Marrink, S. J. *J. Phys. Chem. B* **2008**, *112*, 7438.
- (205) Risselada, H. J.; Marrink, S. J. *J. Phys. Chem. Chem. Phys.* **2009**, *11*, 2056.
- (206) Tieleman, D. P.; Marrink, S.-J. *J. Am. Chem. Soc.* **2006**, *128*, 12462.
- (207) Sapay, N.; Bennett, W. D.; Tieleman, D. P. *Soft Matter* **2009**, *5*, 3295.
- (208) Bennett, W. F. D.; MacCallum, J. L.; Tieleman, D. P. *J. Am. Chem. Soc.* **2009**, *131*, 1972.
- (209) Xing, C. Y.; Faller, R. *J. Chem. Phys.* **2009**, *131*, 175104.
- (210) Finkelstein, A. *Water movement through lipid bilayers, pores, and plasma membranes: Theory and Reality*; Wiley Interscience: New York, 1987.
- (211) Paula, S.; Volkov, A. G.; Deamer, D. W. *Biophys. J.* **1998**, *74*, 319.
- (212) Wilson, M. A.; Pohorille, A. *J. Am. Chem. Soc.* **1996**, *118*, 6580.
- (213) Tepper, H. L.; Voth, G. A. *Biophys. J.* **2005**, *88*, 3095.
- (214) Tepper, H. L.; Voth, G. A. *J. Phys. Chem. B* **2006**, *42*, 21327.
- (215) Khavrutskii, I. V.; Gorfe, A. A.; Lu, B.; McCammon, J. A. *J. Am. Chem. Soc.* **2009**, *131*, 1706.
- (216) Parsegian, V. A. *Nature* **1969**, *221*, 844.
- (217) Jiang, Y.; Lee, A.; Chen, J.; Ruta, V.; Cadene, M.; Chait, B. T.; MacKinnon, R. *Nature* **2003**, *423*, 33.
- (218) Monticelli, L.; Robertson, K. M.; MacCallum, J. L.; Tieleman, D. *FEBS Lett.* **2004**, *564*, 325.
- (219) Tieleman, D. P.; Robertson, K. M.; MacCallum, J. L.; Monticelli, L. *Int. J. Quantum Chem.* **2004**, *100*, 1071.
- (220) Freites, J. A.; Tobias, D. J.; von Heijne, G.; White, S. H. *Proc. Natl. Acad. Sci. U.S.A.* **2005**, *102*, 15059.
- (221) Johansson, A. C. V.; Lindahl, E. *Biophys. J.* **2006**, *91*, 4450.
- (222) Dorairaj, S.; Allen, T. W. *Proc. Natl. Acad. Sci. U.S.A.* **2007**, *104*, 4943.
- (223) MacCallum, J. L.; Bennett, W. F. D.; Tieleman, D. P. *J. Gen. Physiol.* **2007**, *129*, 371.
- (224) MacCallum, J. L.; Bennett, W. F. D.; Tieleman, D. P. *Biophys. J.* **2008**, *94*, 3393.
- (225) Johansson, A. C. V.; Lindahl, E. *Proteins* **2008**, *70*, 1332.
- (226) Li, L.; Vorobyov, I.; Allen, T. W. *J. Phys. Chem. B* **2008**, *112*, 9574.
- (227) Johansson, A. C. V.; Lindahl, E. *J. Phys. Chem. B* **2009**, *113*, 1245.
- (228) Johansson, A. C. V.; Lindahl, E. *J. Chem. Phys.* **2009**, *130*, 185101.
- (229) Boggar, M. B.; Krishnamoorti, R. *Biophys. J.* **2010**, *98*, 586.
- (230) Gurtovenko, A. A.; Anwar, J. *J. Phys. Chem. B* **2007**, *111*, 13379.

- (231) Dzubiella, J.; Allen, R. J.; Hansen, J.-P. *J. Chem. Phys.* **2004**, *120*, 5001.
- (232) Dzubiella, J.; Hansen, J.-P. *J. Chem. Phys.* **2005**, *122*, 234706.
- (233) Wimley, W. C.; Thompson, T. E. *Biochemistry* **1990**, *29*, 1296.
- (234) Bennett, W. F. D.; MacCallum, J. L.; Hinner, M. J.; Marrink, S. J.; Tieleman, D. P. *J. Am. Chem. Soc.* **2009**, *131*, 12714.
- (235) Dressler, V.; Schwister, K.; Haest, C. W. M.; Deuticke, B. *Biochim. Biophys. Acta* **1983**, *732*, 304.
- (236) Vernier, P. T.; Sun, Y.; Marcu, L.; Craft, C. M.; Gundersen, M. A. *FEBS Lett.* **2004**, *572*, 103.
- (237) Vernier, P. T.; Sun, Y.; Marcu, L.; Craft, C. M.; Gundersen, M. A. *Biophys. J.* **2004**, *86*, 4040.
- (238) Gurtovenko, A. A.; Onike, O. I.; Anwar, J. *Langmuir* **2008**, *24*, 9656.
- (239) Neumann, E.; Kakorin, S.; Toensing, K. *Bioelectrochem. Bioenerg.* **1999**, *48*, 3.
- (240) Ginzburg, V. V.; Balijepailli, S. *Nano Lett.* **2007**, *7*, 3716.
- (241) Ali, I.; Yeomans, J. *J. Chem. Phys.* **2005**, *123*, 234903.
- (242) Hoogerbrugge, P. J.; Koelman, J. M. V. A. *Europhys. Lett.* **1992**, *19*, 155.
- (243) Espanol, P.; Warren, P. *Europhys. Lett.* **1995**, *30*, 191.
- (244) Luo, K.; Huopaniemi, I.; Ala-Nissila, T.; Ying, S. C. *J. Chem. Phys.* **2006**, *124*, 114704.
- (245) Panwar, A. S.; Muthukumar, M. *J. Am. Chem. Soc.* **2009**, *131*, 18563.
- (246) Stein, M.; Gabdouliline, R. R.; Wade, R. C. *Curr. Opin. Struct. Biol.* **2007**, *17*, 166.
- (247) Melikov, K. C.; Frolov, V. A.; Shcherbakov, A.; Samsonov, A. V.; Chizmadzhev, Y. A.; Chernomordik, L. V. *Biophys. J.* **2001**, *80*, 1829.
- (248) Harder, E.; MacKerell, A. D.; Roux, B. *J. Am. Chem. Soc.* **2009**, *131*, 2760.
- (249) Yesylevskyy, S. O.; Schäfer, L. V.; Sengupta, D.; Marrink, S. J. *PLoS Comput. Biol.* **2010**, *6*, e1000810.

CR1000783